

# DEUTSCHES ELEKTRONEN-SYNCHROTRON **DESY**

DESY 76/11  
March 1976



Parametrization of the  $q^2$  Dependence of  $\gamma_V$  p Total Cross Sections  
in the Resonance Region

by

F. W. Brasse, W. Flauger, J. Gayler, S. P. Goel,  
R. Haidan, M. Merkwitz and H. Wriedt

2 HAMBURG 52 · NOTKESTIEG 1

To be sure that your preprints are promptly included in the  
**HIGH ENERGY PHYSICS INDEX** ,  
send them to the following address ( if possible by air mail ) :

DESY  
Bibliothek  
2 Hamburg 52  
Notkestieg 1  
Germany.

Parametrization of the  $q^2$  Dependence of  $\gamma_{\nu} p$  Total Cross Sections  
in the Resonance Region

F.W. Brasse, W. Flauger, J. Gayler, S.P. Goel<sup>\*)</sup>,

R. Haidan, M. Merkwitz, H. Wriedt

ABSTRACT

All existing data on  $\gamma_{\nu} p$  total cross sections in the resonance region are fitted in the absolute value of the three momentum transfers  $|\vec{q}|$  independently for small bins of  $W$  in the range  $1.11 \leq W \leq 1.99$  GeV. The data are divided into three ranges of the polarization  $\varepsilon$ :  $\varepsilon \geq 0.9$ ,  $0.9 > \varepsilon > 0.6$ ,  $\varepsilon \leq 0.6$ .

Taking into account statistical and possible systematic errors, a comparison of the fits for different ranges of  $\varepsilon$  indicate that longitudinal contributions to the cross sections in the resonance region are in general small. In the range  $1.3 < W < 1.5$  GeV for  $q^2 > 2$  GeV<sup>2</sup> and above  $W = 1.6$  GeV for  $q^2 > 0.5$  GeV<sup>2</sup> up to 20 % contribution of  $\sigma_{\ell}$  is possible.

<sup>\*)</sup> Now at Kurukshetra University, Kurukshetra, India



## I. INTRODUCTION

The total cross section  $\Sigma$  for the absorption of virtual photons on protons in the region of the main nucleon resonances has been determined in many inelastic electron-proton scattering experiments<sup>1-23)</sup> where only the scattered electron is detected.  $\Sigma$  is written as

$$\Sigma(q^2, W, \epsilon) = \frac{1}{\Gamma_t} \frac{d^2\sigma}{d\Omega dE'} = \sigma_t(W, q^2) + \epsilon \sigma_l(W, q^2) \quad (1)$$

where, as usual<sup>3)</sup>,

$q^2$  is the four-momentum transfer squared,  $W$  the mass of the outgoing hadronic system,  $\Gamma_t$  the flux of transverse polarized virtual photons,  $\epsilon$  the degree of polarization of the virtual photons, and  $\sigma_t$  and  $\sigma_l$  are the absorption cross section for transverse and longitudinal polarized virtual photons, respectively.

A parametrization of the  $q^2$  dependence of the total cross section by a fitting procedure applied to all existing data allows one to study its behaviour with the best available statistics. As the total cross section  $\Sigma$  consists of two parts  $\sigma_t$  and  $\sigma_l$  a parametrization of the measured cross sections  $\Sigma$  has to take into account their variation with  $\epsilon$ . We have divided therefore all data with respect to different regions of  $\epsilon$  and have applied fits to these different sets of cross sections. As a result one gets information of the contributions of  $\sigma_l$  to the total cross section.

First fits of the type presented in this report have been shown earlier<sup>24)</sup> \*. Now some more inelastic e-p scattering data in the resonance region have become available<sup>9-12, 16-18)</sup>. Also, more data<sup>9, 10, 12, 18, 20)</sup> are

---

\* This reference will henceforth be referred to as (I).

now available between  $q^2 = 0$  and  $q^2 = 0.5 \text{ GeV}^2$ , a region in which, earlier, there was generally a lack of data as only a small portion of data from references 2,6,7) belonged to this range. Furthermore, photoproduction data<sup>25)</sup> can now be used for  $q^2 = 0$  in place of the SLAC photon-proton cross sections (used earlier in I) obtained from inelastic electron-proton scattering cross sections by extrapolation to the limit of zero four-momentum transfer<sup>8)</sup>. We have, therefore, done the fitting of the entire electroproduction data available in the resonance region and present the results obtained therefrom in this report. It must be noted however that data for small values of  $\epsilon$  are still very scarce and that there is a need for more measurements.

## 2. THE PROCEDURE OF FITTING

The procedure of fitting is the same as used in (I), which is given below:

The cross section  $\Sigma$  from early results shows the following behaviour<sup>2-6)</sup>:

$$\Sigma = G_D^2(q^2) \cdot A(W) \cdot |\vec{q}|^{b(W)}, \quad (2)$$

where

$G_D^2(q^2)$  = dipole form factor of the nucleon,  
 $\vec{q}$  = three momentum transfer to the hadronic system, and

$A(W)$  and  $b(W)$  are parameters dependent only on  $W$ .

For the validity of eq. (2),  $|\vec{q}|$  must be small as for large values of  $|\vec{q}|$ ,  $\Sigma$  has values smaller than those obtained from the above equation. If the outgoing hadronic system gets a definite total angular momentum, eq. (2) represents the threshold behaviour of  $\Sigma$  for  $|\vec{q}| \rightarrow 0$ . A plot of  $\log(\Sigma/G_D^2)$  vs.  $\log|\vec{q}|$  gives a straight line; quadratic or higher powers of  $\log|\vec{q}|$  may be introduced to account for deviations from this behaviour at high momentum transfers. One additional term is found to be sufficient (I) and, therefore, the following equation is used to fit the data:

$$\log(\Sigma/G_D^2) = a(W) + b(W) \cdot \log(|\vec{q}|/|\vec{q}_0|) + c(W) \cdot \left| \log(|\vec{q}|/|\vec{q}_0|) \right|^{d(W)}, \quad (3)$$

where  $|\vec{q}_0|$  is the value of  $|\vec{q}|$  at  $q^2 = 0$  for the same  $W$ .

The fits done in this work enable us to study the dependence of  $\Sigma$  on  $\epsilon$ . The data with  $\epsilon \geq 0.9$  are taken from references 6 to 12 and 17 to 19 while those with  $\epsilon \leq 0.6$  from references 3 to 5, 8, 9, 11, 19, and 20. For the fit in the range  $0.6 < \epsilon < 0.9$ , the relevant data from the above mentioned references as well as from ref. (2) are used. In  $W$  the fits were restricted to the range  $1.11 \leq W \leq 1.99$  GeV. The Daresbury photoproduction cross sections<sup>25)</sup>, having  $W$  in the relevant range, have been included in all  $\epsilon$  ranges as  $\sigma_\rho$  is zero at  $q^2 = 0$ . We have used two bin sizes for  $W$ , one,  $\Delta W = 0.015$  GeV, across the bumps of the resonances up to  $W = 1.755$  GeV, and the other,  $\Delta W = 0.020$  GeV, for  $1.770 \leq W \leq 1.990$ .

The errors as given in the various references have been increased to include possible systematic errors, since most of the papers give only statistical errors. Furthermore, the final bin size in  $W$  introduces an error which is not negligible around the resonances where the cross section changes rapidly with  $W$ . Finally, there may be differences in the absolute normalization of the measurements from different experimental arrangements. Therefore, to the errors of the cross sections in the range  $\epsilon \geq 0.9$  with  $W > 1.755$  GeV a 5 % error has been added quadratically, to all others a 10 % error. Using the above errors the cross sections resulting from the fits were practically not different from those, where only the original errors were used.

### 3. RESULTS

Most of the additional data (9-12, 17, 18, 20) available after the completion of (I) belong to the range  $\epsilon \geq 0.9$ , and therefore the results of this work for the range  $\epsilon \leq 0.6$  are not very different from the corresponding results given in (I).

### 3.1 The parameter $d$

---

For the range  $\epsilon \leq 0.6$  the amount of data is not sufficient to determine the four parameters in eq. (3) for each  $W$  bin. Further,  $b$  and  $c$  cannot be separated if  $d$  is around 1. This happens for some  $W$  bins in the case  $\epsilon \leq 0.6$ , when cross sections for high values of  $q^2$  are missing or when the errors are too large. Therefore in a first step  $d$  was left free for  $\epsilon \geq 0.9$  only. From these fits an average value of  $d = 3.0$  for all bins of  $W$  and all ranges of  $\epsilon$  was taken for the final fits. The choice of  $d$  turned out not to be critical for the cross sections resulting from the fits.

### 3.2 Coefficients $a$ , $b$ and $c$

---

The values of the coefficients  $a$ ,  $b$  and  $c$  as well as their errors and correlations as determined from the least squares fits of eq. (3) are given in Tables I, II, and III for the three ranges of  $\epsilon$ . Also given are the weighted average values of  $\epsilon$  for each  $W$  bin, the  $\chi^2$  per degree of freedom and the number of degrees of freedom.

### 3.3 Behaviour of the fits as a function of $|\vec{q}|^2$

---

In figs. 1 to 6 the measured values of  $\Sigma/G_D^2$  are shown as a function of  $|\vec{q}|^2$  separately for the two extreme ranges of  $\epsilon$  for six values of  $W$ , i.e., for  $W = 1.230, 1.380, 1.530, 1.605, 1.695,$  and  $1.890$  GeV. Also shown for each  $W$  value is the scale of  $q^2$ . As mentioned in sec. 1, there are now available some experimental data for the range  $\epsilon \geq 0.9$ , between  $q^2 = 0$  and  $q^2 = 0.5 \text{ GeV}^2$ , as can be seen from figs. 1 to 6.

Besides the experimental cross sections we have also shown the fit for the two ranges of  $\epsilon$  for each value of  $W$  in figs. 1-6. The fits at  $W = 1.230, 1.530$  and  $1.605$  for both ranges of  $\epsilon$  almost pass through the photoproduction experimental points (Fig. 1,3 and 4). The fits at  $W = 1.380$  GeV pass below, while those at  $W = 1.695$  and  $1.890$  GeV pass



above the corresponding experimental points but generally touching or passing through the error bars. It should, however, be pointed out that for  $\epsilon \leq 0.6$  there are no experimental data below  $q^2 = 0.5$  to guide the fit while for  $\epsilon \geq 0.9$  the expression used to obtain the fit is somewhat inadequate to account for a  $\sigma_{\ell}$  contribution restricted to small values of  $q^2$ .

The corresponding results for  $0.6 < \epsilon < 0.9$  are shown in Figs. 7 to 9. The behaviour of the fits for the three ranges of  $\epsilon$  is practically the same. Also, the inclusion or non-inclusion of the photoproduction data does not affect the behaviour of the fits in any appreciable manner.

### 3.4 Dependence of $\Sigma$ on $W$ and $q^2$

---

In Figs. 10-18 we show the cross section  $\Sigma$  for fixed values of  $q^2$ , i.e.,  $q^2 = 0.1, 0.3, 0.5, 1.0, 2.0, 3.0, 4.0, 5.0$  and  $6.0 \text{ GeV}^2$  across the range  $1.110 \leq W \leq 1.990 \text{ GeV}$  as computed from our fits. Whereas for  $q^2 < 0.5 \text{ GeV}^2$  we only show results for  $\epsilon \geq 0.9$ , in the figures for  $q^2 \geq 0.5 \text{ GeV}^2$  the values of  $\Sigma$  are compared for the two extreme ranges of  $\epsilon$ . The errors are calculated with the complete error matrix of the coefficients  $a$ ,  $b$  and  $c$  according to the following expression:

$$(\Delta\Sigma)^2 = (\Delta a)^2 \cdot \left(\frac{\delta\Sigma}{\delta a}\right)^2 + (\Delta b)^2 \cdot \left(\frac{\delta\Sigma}{\delta b}\right)^2 + (\Delta c)^2 \cdot \left(\frac{\delta\Sigma}{\delta c}\right)^2 - 2 \cdot C_{ab} \cdot \frac{\delta\Sigma}{\delta a} \cdot \frac{\delta\Sigma}{\delta b} + 2 \cdot C_{ac} \cdot \frac{\delta\Sigma}{\delta a} \cdot \frac{\delta\Sigma}{\delta c} - 2 \cdot C_{bc} \cdot \frac{\delta\Sigma}{\delta b} \cdot \frac{\delta\Sigma}{\delta c},$$

where  $\Delta a$ ,  $\Delta b$ ,  $\Delta c$ ,  $C_{ab}$ ,  $C_{ac}$  and  $C_{bc}$  are the coefficients of the error matrix as given in tables I, II and III.

We think that the fits are not sufficient to calculate cross sections beyond  $q^2 = 4.0 \text{ GeV}^2$  for  $\epsilon \leq 0.6$  and beyond  $q^2 = 6.0 \text{ GeV}^2$  for  $\epsilon \geq 0.9$ .

The results show the faster decrease of the first resonance with increasing  $q^2$  compared to the nonresonant background around this resonance and compared to the two other bumps of resonances around 1.5 and 1.67 GeV.

The second bump on the contrary increases slightly in relation to the background at the same energy with increasing  $q^2$  whereas the third one stays practically constant. The position of the third bump moves to higher energies with increasing  $q^2$  as has been noticed earlier<sup>18)</sup>.

### 3.5 The Ratio $R = \sigma_\ell / \sigma_t$

The difference between  $\Sigma_{\epsilon \leq 0.9}$  and  $\Sigma_{\epsilon \geq 0.6}$  is a direct measure of  $\sigma_\ell$  and is very close to  $\frac{1}{2} \cdot \sigma_\ell$  (eq.1), since the average values of  $\epsilon$  in the two cases are close to 1.0 and 0.5 (Tables I and III). Therefore, the comparison of  $\Sigma$  for the two ranges of  $\epsilon$  in the Figs. 12-15 allows one to determine  $\sigma_\ell$ . There are systematic differences outside the error bars between the two sets of cross sections. For  $q^2 = 0.5 \text{ GeV}^2$  with  $W < 1.5 \text{ GeV}$  the difference  $\Sigma_{\geq 0.9} - \Sigma_{\leq 0.6}$  has unphysical values. This is most likely due to the uncertainty of the fit for  $\epsilon < 0.6$  for small values of  $q^2$  because of lack of data. It also may show the problem of estimating systematic errors for the different set of measurements, measured with different experimental arrangements. The same conclusion could be made for  $W > 1.6 \text{ GeV}$  and small  $q^2$  values, where  $\Sigma_{\epsilon \leq 0.6}$  is systematically smaller than  $\Sigma_{\epsilon \geq 0.9}$ . However there the difference stays on to larger values of  $q^2$  up to  $3 \text{ GeV}^2$ , indicating a possible longitudinal contribution of about 10-20 %. This is consistent with a direct determination of  $R$  at  $q^2 = 1 \text{ GeV}^2$  11).

For  $W < 1.6 \text{ GeV}$  and  $0.5 < q^2 < 2 \text{ GeV}^2$  no difference outside the error bars between the two sets of measurement is visible except for a small effect on the sides of the first resonance, which might be due to uncertainties in the energy  $W$ . A 10 % contribution of  $\sigma_\ell$  at the first resonance around  $q^2 = 0.5 \text{ GeV}^2$  is indicated by direct determinations<sup>20,21)</sup>. Above  $q^2 = 2 \text{ GeV}^2$  and for  $1.3 < W < 1.5 \text{ GeV}$  a longitudinal contribution of about 20 % is not excluded.

LIST OF TABLES

Table I: Results of the fits for  $\varepsilon \geq 0.9$

Table II: Results of the fits for  $0.9 > \varepsilon > 0.6$

Table III: Results of the fits for  $\varepsilon \leq 0.6$

REFERENCES

1. H.L. Lynch, J.W. Allaby and D.M. Ritson, HEPL-494 B (1967)
2. A.A. Cone, K.W. Chen, J.R. Dunning, G. Hartwig, N.F. Ramsey, J.K. Walker, R. Wilson, Phys. Rev. 156 (1967) 1490
3. F.W. Brasse, J. Engler, E. Ganßauge, M. Schweitzer, Nuovo Cim. X, 55A, 679 (1968) and DESY 67/34 (1967)
4. W. Albrecht, F.W. Brasse, H. Dorner, W. Flauger, K.-H. Frank, J. Gayler, H. Hultschig, J. May, E. Ganßauge, Phys. Lett. 28B (1968) 225 and DESY 68/48 (1968)
5. W. Albrecht, F.W. Brasse, H. Dorner, W. Flauger, K.-H. Frank, J. Gayler, H. Hultschig, J. May, E. Ganßauge, Nucl. Phys. B13, (1969) 1 and DESY 69/7
6. W. Bartel, B. Dudelzak, H. Krehbiel, J. McElroy, U. Meyer-Berkhout, W. Schmidt, V. Walther, G. Weber, Phys. Lett. 28B (1968) 148;  
W. Bartel, thesis, DESY internal report F22-69/3 (1969)
7. E.D. Bloom, G. Buschhorn, R.L. Cottrell, D.H. Coward, H. De Staebler, J. Drees, C.L. Jordon, G. Miller, L. Mo, H. Piel, R.E. Taylor, M. Breidenbach, W.R. Ditzler, J.I. Friedman, G.C. Hartmann, H.W. Kendall, J.S. Pucher, SLAC-PUB-795 (1970);  
M. Breidenbach, Thesis; R.E. Taylor, private communication
8. E.D. Bloom, R.L. Cottrell, D.H. Coward, H. DeStaebler, Jr., J. Drees, G. Miller, L.W. Mo, R.E. Taylor, J.I. Friedman, G.C. Hartmann, and H.W. Kendall, SLAC-PUB 653 (1969)
9. J. Moritz, K.H. Schmidt, D. Wegener, J. Bleckwenn and E. Engles, Jr. DESY 71/61; Nucl. Phys. B41 (1972) 336
10. J. Bleckwenn, thesis, DESY internal report F23-71/2 (1971)
11. J.-C. Alder, F.W. Brasse, E. Chazelas, W. Fehrenbach, W. Flauger, K.-H. Frank, E. Ganßauge, J. Gayler, W. Krechlok, V. Korbel, J. May, M. Merkwitz, P.D. Zimmerman, Nucl. Phys. B48 (1972), 487 and DESY 72/38 (1972)

12. M. Köbberling, J. Moritz, K.H. Schmidt, D. Wegener, D. Zeller, J. Bleckwenn, F.H. Heimlich, Karlsruhe KFK 1822; Nucl. Phys. B82 (1974) 201
13. E.D. Bloom, D.H. Coward, H. DeStaebler, J. Drees, G. Miller, L.W. Mo, R.E. Taylor, M. Breidenbach, J.I. Friedman, G.C. Hartmann, H.W. Kendall, Phys. Rev. Lett. 23 (1969) 930
14. M. Breidenbach, J.I. Friedman, H.W. Kendall, E.D. Bloom, D.H. Coward, H. DeStaebler, J. Drees, L.W. Mo, and R.E. Taylor, Phys. Rev. Lett. 23 (1969) 935
15. G. Miller, E.D. Bloom, G. Buschhorn, D.H. Coward, H. DeStaebler, J. Drees, C.L. Jordan, L.W. Mo, R.E. Taylor, J.I. Friedman, G.C. Hartmann, H.W. Kendall and R. Verdier, Phys. Rev. D5 (1972) 528
16. J.S. Poucher, M. Breidenbach, R. Ditzler, J.I. Friedman, H.W. Kendall, E.D. Bloom, R.L.A. Cottrell, D.H. Coward, H. DeSteblor, C.L. Jordan, H. Piel, and R.E. Taylor, SLAC PUB 1309 (1973); Phys. Rev. Lett. 32 (1974) 118
17. Arie Bodek, Ph. D. thesis, MIT (1972);  
Edard M. Riordan, Ph. D. thesis, MIT (1973) and also private communication
18. S. Stein, W.B. Atwood, E.D. Bloom, R.L.A. Cottrell, H. DeSteabler, C.L. Jordan, H.G. Piel, C.Y. Prescott, R. Siemann, R.E. Taylor, SLAC-PUB-1528 (1975)
19. W. Bartel, B. Dudelzak, H. Krehbiel, J. McElroy, U. Meyer-Berkhout, W.Schmidt, V. Walter, G. Weber, Phys. Lett. 27B (1968) 660
20. W. Bartel, F.W. Büsler, W.R. Dix, R. Felst, D. Harms, H. Krehbiel, P.E. Kuhlmann, J. McElroy, J. Meyer, G. Weber, Phys. Lett. 35B (1971) 181 and W.R. Dix, Thesis, Universität Hamburg (1971)
21. K. Bätzner, U. Beck, K.H. Becks, C. Berger, J. Drees, G. Knop, M. Leenen, K. Moser, C. Nietzel, E. Schlösser, H.E. Stier, Phys. Lett. 39B(1972) 575
22. W.Albrecht, F.W. Brasse, H. Dorner, W. Flauger, K.-H. Frank, J. Gayler, H. Hultschig, V. Korbel, J. May, DESY 69/46 (1969)

23. E.M. Riordan, A. Bodek, M. Breidenbach, D.L. Dubin, J.E. Elias, J.I. Friedman, H.W. Kendall, J.S. Poucher, M.R. Sogard, D.H. Coward, SLAC-PUB 1417 (1974)
24. F.W. Brasse, W. Fehrenbach, W. Flauger, K.-H. Frank, J. Gayler, V. Korbel, J. May, P.D. Zimmerman and E. Ganßauge, DESY 71/2 (1971)
25. T.A. Armstrong, W.R. Hogg, G.M. Lewis, A.W. Robertson, G.R. Brookes, A.S. Clough, J.H. Freeland, W. Galbraith, A.F. King, W.R. Rawlinson, N.R.S. Tait, J.C. Thompson and D.W.L. Tolfree, Daresbury DNPL/P 88 (1971)

FIGURE CAPTIONS

Fig. 1:  $\Sigma/G_D^2$  as a function of  $|\vec{q}|^2$  in a double logarithmic plot for  $W = 1.230$  GeV and with  $d = 3.0$ . Shown is also the scale of  $q^2$ . The curves are our fit with eq. (2) and with the parameters in tables I and III.

For  $\epsilon \geq 0.9$ , error bars are given for extreme positions while for  $\epsilon \leq 0.6$ , they are given for each data point.

Fig. 2: same as 1, but for  $W = 1.380$  GeV

Fig. 3: same as 1, but for  $W = 1.530$  GeV

Fig. 4: same as 1, but for  $W = 1.605$  GeV

Fig. 5: same as 1, but for  $W = 1.695$  GeV

Fig. 6: same as 1, but for  $W = 1.890$  GeV

Fig. 7: same as 1, but for  $0.6 < \epsilon < 0.9$ ,  $W = 1.230$  and  $1.380$  GeV

Fig. 8: Same as 7, but for  $W = 1.530$  and  $1.605$  GeV

Fig. 9: same as 7, but for  $W = 1.695$  and  $1.890$  GeV

Fig. 10:  $\Sigma$  calculated from our fits for  $\epsilon \geq 0.9$  as a function of  $W$  for  $q^2 = 0.1$  GeV<sup>2</sup>

Fig. 11: Same as 10, but for  $q^2 = 0.3$  GeV<sup>2</sup>

Fig. 12:  $\Sigma$  calculated from our fits for  $\epsilon \geq 0.9$  and  $\epsilon \leq 0.6$ , as a function of  $W$  for  $q^2 = 0.5$  GeV<sup>2</sup>

Fig. 13: same as 12, but for  $q^2 = 1.0$  GeV<sup>2</sup>

Fig. 14: same as 12, but for  $q^2 = 2.0$  GeV<sup>2</sup>

Fig. 15: same as 12, but for  $q^2 = 3.0$  GeV<sup>2</sup>

Fig. 16: same as 12, but for  $q^2 = 4.0$  GeV<sup>2</sup>

Fig. 17:  $\Sigma$  calculated from our fits for  $\epsilon \geq 0.9$  as a function of  $W$  for  $q^2 = 5.0$  GeV<sup>2</sup>

Fig. 18: same as 17, but for  $q^2 = 6.0$  GeV<sup>2</sup>

W	$\epsilon$	a	b	$(\Delta b)^2 \cdot 10^4$	c	$(\Delta c)^2 \cdot 10^4$	$C_{ab} \cdot 10^4$	$C_{ac} \cdot 10^4$	$C_{bc} \cdot 10^4$	$\chi^2$	NF
1.119	0.963	5.045	251.7	217.3	0.043	2.9	228.2	23.5	23.8	2.3	57
1.125	0.962	5.126	163.5	166.4	0.024	2.9	163.5	18.9	20.3	2.3	70
1.140	0.963	5.350	109.8	116.0	0.000	2.3	110.1	13.5	15.4	2.2	71
1.155	0.956	5.621	83.1	95.9	-0.013	2.0	86.0	11.1	13.1	2.2	71
1.170	0.955	5.913	42.5	51.8	-0.023	1.4	44.5	5.9	7.8	1.3	69
1.185	0.957	5.955	45.3	58.1	-0.069	1.5	49.6	6.8	8.7	1.1	83
1.200	0.960	6.139	31.8	46.0	-0.060	1.5	36.4	5.4	7.6	1.0	75
1.215	0.956	6.178	26.7	39.7	-0.030	1.4	31.0	4.7	6.7	0.9	83
1.230	0.961	6.125	27.3	43.9	-0.065	1.8	32.6	5.2	7.9	0.7	55
1.245	0.960	5.959	23.1	37.9	-0.056	1.5	28.0	4.4	6.8	0.8	80
1.260	0.955	5.769	25.5	46.7	-0.065	2.3	32.8	5.5	9.3	1.3	83
1.275	0.962	5.622	21.5	43.0	-0.050	2.4	23.6	5.3	9.0	1.1	80
1.305	0.960	5.431	22.0	42.0	-0.043	2.4	28.5	5.1	8.7	1.5	76
1.320	0.957	5.175	17.1	42.1	-0.054	3.2	25.0	5.3	10.2	1.3	85
1.350	0.958	5.003	15.7	38.6	-0.040	3.2	22.3	4.9	9.6	1.4	90
1.365	0.954	5.065	16.0	58.3	-0.040	5.6	33.5	7.9	15.8	1.6	76
1.380	0.957	5.345	15.7	44.3	-0.015	4.4	24.6	7.9	12.1	1.5	86
1.395	0.957	5.078	13.9	43.5	-0.029	4.2	24.0	5.4	11.5	1.3	77
1.410	0.960	5.145	10.0	40.1	-0.043	3.4	21.5	4.4	9.7	1.3	71
1.425	0.957	5.156	14.8	50.1	-0.032	5.9	25.5	6.5	16.8	0.3	75
1.440	0.957	5.234	10.6	47.2	-0.040	5.4	24.3	6.0	13.4	1.0	79
1.455	0.955	5.258	15.4	54.1	-0.084	6.2	27.5	6.3	15.4	0.9	67
1.470	0.958	5.371	15.0	51.5	-0.115	7.1	26.0	7.0	16.1	0.8	75
1.485	0.956	5.457	15.3	54.3	-0.105	7.6	26.1	7.1	17.2	0.8	67
1.500	0.956	5.243	15.4	51.6	-0.154	5.4	25.0	6.3	14.1	0.8	69
1.515	0.957	5.219	14.7	54.7	-0.164	8.5	27.3	7.4	13.3	0.5	65
1.530	0.956	5.405	16.6	54.7	-0.181	7.5	26.1	7.1	17.1	0.3	65
1.545	0.957	5.354	16.6	59.1	-0.220	7.4	23.7	7.5	17.6	0.5	55
1.560	0.955	5.341	10.7	70.1	-0.220	12.9	31.3	7.6	24.5	0.5	59
1.575	0.954	5.320	14.6	58.9	-0.245	8.4	26.8	7.3	18.4	0.5	65
1.590	0.955	5.275	17.0	77.2	-0.233	16.9	31.1	10.2	29.1	0.5	57
1.605	0.955	5.250	10.9	77.2	-0.233	17.0	33.5	10.6	30.1	0.5	51
1.620	0.954	5.330	15.7	75.4	-0.332	14.4	32.2	9.5	27.1	0.6	51
1.635	0.956	5.375	15.3	91.6	-0.299	19.9	32.0	11.0	33.1	0.7	50
1.650	0.955	5.423	14.9	72.8	-0.319	14.4	32.0	9.2	26.6	0.4	52
1.665	0.954	5.478	14.3	84.3	-0.383	22.1	31.5	11.2	35.1	0.4	51
1.680	0.955	5.443	14.2	72.5	-0.393	14.9	28.5	7.0	27.1	0.4	50
1.695	0.953	5.350	13.7	60.8	-0.460	21.3	29.3	10.7	34.7	0.4	43
1.710	0.953	5.335	13.8	80.1	-0.534	23.0	29.1	10.6	34.5	0.4	48
1.725	0.955	5.256	14.2	82.0	-0.522	19.0	29.5	10.1	33.0	0.5	46
1.740	0.953	5.223	13.6	81.6	-0.574	21.2	29.8	10.7	34.8	0.4	48
1.755	0.960	5.154	5.4	42.4	-0.727	23.8	13.0	6.2	40.6	0.3	46
1.770	0.959	5.149	4.9	37.3	-0.625	16.8	11.5	4.9	19.5	0.7	45
1.790	0.960	5.143	4.0	32.2	-0.704	17.7	9.8	4.6	18.8	0.8	60
1.810	0.957	5.125	3.8	33.4	-0.856	21.0	9.5	4.7	20.6	0.8	52
1.830	0.954	5.158	3.6	29.0	-0.798	11.2	9.7	3.6	14.4	1.1	65
1.850	0.955	5.159	3.8	38.2	-1.048	40.2	10.2	6.1	30.0	0.9	59
1.870	0.958	5.178	3.7	37.1	-0.980	29.0	9.3	6.1	24.9	1.1	61
1.890	0.961	5.182	3.5	35.1	-1.021	29.0	9.1	4.9	23.5	1.4	55
1.910	0.955	5.155	3.4	34.7	-1.092	23.9	9.1	4.7	22.3	1.7	56
1.930	0.956	5.160	3.9	42.5	-1.313	39.2	10.9	6.5	31.5	1.0	57
1.950	0.956	5.155	3.2	37.8	-1.341	40.3	9.2	5.7	29.9	1.4	61
1.970	0.954	5.163	3.4	40.6	-1.266	34.5	9.9	5.3	29.4	1.3	61
1.990	0.953	5.172	4.3	50.9	-1.473	49.1	12.6	8.1	39.4	1.1	56

Table I: Results of the fits for  $\epsilon \geq 0.9$



W	$\epsilon$	a	$(\Delta a)^2 \cdot 10^4$	b	$(\Delta b)^2 \cdot 10^4$	c	$(\Delta c)^2 \cdot 10^4$	$C_{ab} \cdot 10^4$	$C_{ac} \cdot 10^4$	$C_{bc} \cdot 10^4$	$\chi^2$	NF
1.110	0.835	-0.050	16677.8	4.849	9928.3	-0.285	73.8	12807.8	1060.6	838.0	2.3	18
1.125	0.820	1.082	9586.8	4.120	5790.4	-0.100	42.8	7415.9	610.8	486.4	1.7	19
1.140	0.837	4.119	3435.7	2.244	2468.2	-0.100	24.6	2895.1	272.3	238.1	2.5	24
1.155	0.859	3.898	2482.6	2.824	1864.3	-0.155	20.9	2135.3	209.8	189.3	1.5	21
1.170	0.854	5.990	90.1	1.257	90.9	-0.006	3.5	79.5	7.6	13.7	3.0	19
1.185	0.844	6.033	1077.1	1.548	910.2	-0.025	11.5	982.8	101.6	97.3	1.6	25
1.200	0.854	6.160	85.7	1.730	93.6	-0.066	3.5	82.1	9.9	13.9	0.8	22
1.215	0.857	6.219	84.6	1.805	95.1	-0.086	4.0	82.5	9.6	15.1	0.5	25
1.230	0.864	6.117	81.6	1.866	97.5	-0.071	2.5	84.3	10.4	13.7	1.1	28
1.245	0.859	5.959	77.9	1.914	82.8	-0.054	1.5	75.8	7.7	9.5	1.1	24
1.260	0.851	5.451	584.1	2.272	723.0	-0.084	15.8	645.1	89.9	103.2	0.8	31
1.275	0.848	5.675	79.8	1.840	121.0	0.012	4.9	92.4	13.6	20.3	1.6	26
1.290	0.858	5.417	85.8	2.102	127.6	-0.037	5.4	96.8	14.2	22.4	1.2	23
1.305	0.845	5.238	82.2	2.221	134.1	-0.046	7.0	98.4	15.9	25.7	1.3	23
1.320	0.781	5.084	71.9	2.368	105.8	-0.058	2.7	81.7	10.4	15.1	1.7	28
1.335	0.783	4.913	57.5	2.622	76.1	-0.085	1.0	62.3	5.6	7.5	1.9	31
1.350	0.798	4.458	407.6	3.146	695.2	-0.131	25.1	528.1	93.7	127.3	0.9	26
1.365	0.856	5.012	69.0	2.537	148.3	-0.031	10.3	71.7	17.5	34.0	1.1	19
1.380	0.859	5.128	86.1	2.473	172.3	-0.031	9.8	111.5	20.0	35.3	1.4	18
1.395	0.851	5.140	75.9	2.533	158.3	-0.031	13.6	101.1	20.3	38.5	1.7	22
1.410	0.828	5.261	38.2	2.610	67.4	-0.093	2.2	46.2	6.0	10.2	1.7	26
1.425	0.853	5.370	44.7	2.461	121.3	-0.000	13.5	66.1	15.6	34.9	1.3	26
1.440	0.851	5.416	42.3	2.570	114.9	-0.052	11.5	62.3	14.1	31.5	1.2	24
1.455	0.788	5.466	24.5	2.700	77.7	-0.083	8.1	38.5	9.0	21.8	0.7	33
1.470	0.824	5.508	30.2	2.799	97.0	-0.104	10.4	47.7	11.5	27.9	0.9	27
1.485	0.847	5.578	29.6	2.929	102.4	-0.104	13.0	49.2	12.9	31.8	0.9	30
1.500	0.839	5.629	29.4	3.016	111.7	-0.096	19.7	50.7	14.7	39.8	0.9	27
1.515	0.847	5.623	20.4	3.128	71.3	-0.163	7.1	33.1	7.6	19.6	0.9	33
1.530	0.841	5.555	23.2	3.215	103.4	-0.173	22.2	43.3	14.3	41.2	0.5	34
1.545	0.851	5.503	24.4	3.271	118.3	-0.192	26.0	46.5	15.5	48.1	0.6	26
1.560	0.852	5.471	19.1	3.288	90.7	-0.191	18.3	35.5	11.3	35.5	0.7	32
1.575	0.819	5.419	21.8	3.328	117.0	-0.202	29.0	43.7	15.9	51.2	0.7	30
1.590	0.846	5.390	21.5	3.390	109.6	-0.239	23.3	42.3	14.1	43.5	0.5	30
1.605	0.845	5.423	17.9	3.576	110.9	-0.168	34.2	37.7	14.7	53.2	0.6	31
1.620	0.840	5.396	18.6	3.567	106.6	-0.286	27.1	39.4	14.2	47.2	0.6	33
1.635	0.765	5.451	12.7	3.600	50.5	-0.239	2.6	21.3	3.5	9.7	0.6	36
1.650	0.836	5.400	18.4	3.595	136.6	-0.408	36.3	43.4	17.3	62.3	0.5	31
1.665	0.827	5.446	16.3	4.046	127.4	-0.402	48.4	38.4	15.8	67.3	0.5	30
1.680	0.690	5.448	13.1	4.124	63.5	-0.355	5.9	24.2	5.2	16.2	0.5	34
1.695	0.813	5.421	12.7	4.270	78.7	-0.400	10.9	26.5	7.2	24.8	0.4	35
1.710	0.818	5.398	20.5	4.667	161.0	-0.603	52.2	50.5	22.5	81.9	0.4	32
1.725	0.801	5.248	19.9	4.818	150.7	-0.642	46.5	47.9	21.0	75.7	0.3	33
1.740	0.814	5.193	16.0	4.856	122.9	-0.637	31.1	38.0	14.4	53.9	0.3	33
1.755	0.818	5.099	9.0	5.069	74.0	-0.773	27.9	22.6	10.8	40.7	0.7	29
1.770	0.819	5.076	9.8	5.112	82.0	-0.768	41.7	24.9	13.3	51.4	0.8	29
1.790	0.810	5.054	9.3	5.236	72.7	-0.879	33.8	23.2	12.2	44.2	0.6	35
1.810	0.821	5.064	8.4	5.331	74.5	-0.941	38.3	21.8	11.8	47.3	0.9	31
1.830	0.818	5.028	13.4	5.609	109.5	-1.075	53.0	34.8	19.4	68.7	0.9	27
1.850	0.823	5.080	9.7	5.628	86.7	-1.118	45.9	25.1	14.0	56.8	1.1	24
1.870	0.823	5.076	14.3	5.819	146.4	-1.223	85.6	40.9	25.2	101.5	0.6	20
1.890	0.775	5.173	9.4	5.461	60.4	-0.812	12.5	20.0	6.8	24.4	3.9	20
1.910	0.833	5.011	13.5	6.391	160.0	-1.581	103.7	40.2	25.0	114.4	0.4	15
1.930	0.811	5.136	19.2	5.995	156.6	-1.219	60.2	49.0	25.0	89.8	1.7	15
1.950	0.781	5.055	14.1	6.455	184.0	-1.605	132.1	43.7	29.3	141.6	2.1	14
1.970	0.648	5.035	14.1	6.565	154.2	-1.055	19.7	40.9	12.4	50.3	1.1	15
1.990	0.826	5.059	16.8	7.063	1167.1	-4.060	39509.2	104.7	421.2	6320.8	0.5	15

Table II: Results of the fits for  $0.9 > \epsilon > 0.6$

W	$\epsilon$	a	$(\Delta a)^2 \cdot 10^4$	b	$(\Delta b)^2 \cdot 10^4$	c	$(\Delta c)^2 \cdot 10^4$	$C_{ab} \cdot 10^4$	$C_{ac} \cdot 10^4$	$C_{bc} \cdot 10^4$	$\chi^2$	NF
1.110	0.488	-3.024	2132.4	6.513	10961.8	-0.350	49.5	15645.2	1014.9	128.0	2.0	8
1.125	0.461	3.795	30057.5	1.935	19307.3	-0.605	153.2	24049.8	2113.8	1707.9	1.5	10
1.140	0.455	6.003	15772.4	0.774	10174.7	0.036	83.0	12622.9	1112.6	907.7	2.2	10
1.155	0.473	6.339	2102.8	0.653	1420.6	0.054	9.7	1714.5	134.7	114.1	2.6	11
1.170	0.499	6.071	92.2	1.917	113.2	0.073	3.9	81.7	9.6	19.3	1.0	14
1.185	0.429	6.234	4390.1	0.709	4387.4	0.023	80.5	4372.0	577.7	586.9	1.4	15
1.200	0.498	6.166	37.5	1.699	97.4	-0.054	2.7	31.6	9.0	14.0	1.4	15
1.215	0.450	5.239	30.6	1.769	87.8	-0.059	2.2	77.7	8.2	11.4	0.4	18
1.230	0.498	6.149	88.0	1.929	120.7	-0.067	4.7	34.4	10.1	20.9	0.2	11
1.245	0.444	5.988	90.5	1.942	156.9	-0.060	11.0	174.3	19.1	36.0	0.7	15
1.260	0.479	5.155	455.3	2.703	537.9	-0.158	11.9	486.6	65.8	76.1	0.6	19
1.275	0.460	5.727	81.2	1.892	128.1	-0.017	5.5	92.4	14.4	24.6	0.8	18
1.290	0.475	5.454	37.9	1.932	176.7	0.064	12.6	112.0	21.3	42.1	0.5	17
1.305	0.439	5.262	77.4	2.244	118.7	-0.050	4.6	88.0	12.6	20.2	1.1	19
1.320	0.455	5.200	87.1	2.040	198.9	0.071	17.8	118.1	25.6	53.2	1.1	18
1.335	0.431	5.153	37.4	1.783	246.2	-0.129	32.2	136.7	33.3	77.5	0.8	15
1.350	0.423	4.365	219.7	3.205	362.4	-0.155	14.1	273.3	47.3	67.0	0.7	23
1.365	0.475	5.168	39.7	2.100	523.7	0.159	52.5	145.5	39.9	125.5	0.5	11
1.380	0.434	5.102	33.0	2.537	195.7	-0.136	19.9	113.7	21.6	53.5	1.2	12
1.395	0.452	5.172	33.0	2.473	153.5	-0.044	11.9	133.4	14.4	34.3	1.1	13
1.410	0.478	5.332	38.9	3.493	34.2	-0.171	2.0	76.5	7.2	11.1	0.6	12
1.425	0.471	5.373	36.5	2.537	297.0	0.035	6.7	133.3	36.3	123.1	0.6	11
1.440	0.459	5.396	60.3	2.581	170.0	-0.059	15.8	133.3	20.2	43.3	1.0	14
1.455	0.433	5.435	35.9	2.324	238.2	-0.171	55.7	135.6	52.2	125.2	1.0	13
1.470	0.463	5.564	91.0	2.599	235.6	-0.098	43.5	120.9	27.2	83.3	0.5	10
1.485	0.445	5.515	37.1	2.371	185.3	-0.102	23.1	112.0	21.8	49.9	0.8	12
1.500	0.477	5.574	37.0	3.407	243.6	-0.216	52.2	124.1	30.4	95.1	1.6	10
1.515	0.439	5.550	30.3	3.322	203.8	-0.181	31.7	117.5	23.2	63.1	0.2	9
1.530	0.452	5.470	90.6	3.375	292.7	-0.162	68.7	135.3	37.4	114.6	0.5	9
1.545	0.477	5.317	35.3	3.750	324.4	-0.195	35.1	137.2	39.1	147.2	0.1	7
1.560	0.430	5.349	31.0	3.750	178.4	-0.255	16.1	111.1	18.3	39.4	0.3	12
1.575	0.435	5.311	30.2	3.559	332.8	-0.182	138.3	143.5	45.1	197.0	0.6	7
1.590	0.414	5.315	93.0	4.143	333.0	-0.272	62.0	136.3	33.0	112.5	0.7	7
1.605	0.436	5.373	92.6	4.100	405.3	-0.425	100.8	147.6	40.6	156.0	0.2	5
1.620	0.452	5.433	73.3	4.035	405.2	-0.288	11.1	113.9	15.8	35.0	1.4	9
1.635	0.417	5.235	63.7	4.687	356.0	-0.351	11.1	151.5	53.7	161.0	0.7	10
1.650	0.471	5.243	36.4	4.732	1038.0	-0.521	134.2	151.5	154.9	1302.4	0.4	5
1.675	0.421	5.160	86.0	4.782	470.9	-0.559	150.1	177.2	71.1	232.5	0.3	9
1.700	0.470	5.371	82.1	5.215	753.7	-0.341	543.4	207.7	112.0	559.6	1.0	6
1.725	0.456	5.072	49.9	5.050	308.0	-0.716	93.7	59.1	23.4	114.3	0.5	13
1.750	0.435	5.071	31.4	5.061	271.0	-0.345	44.4	66.8	18.3	102.4	1.4	7
1.775	0.457	5.030	27.0	4.679	105.0	-0.474	7.7	42.5	7.1	22.1	1.5	14
1.800	0.451	4.835	15.3	5.332	210.1	-0.460	105.1	38.0	20.4	170.1	1.0	15
1.825	0.459	4.976	32.4	5.959	333.5	-1.124	504.6	59.7	53.3	373.1	1.3	13
1.850	0.418	5.021	15.3	5.977	211.4	-1.368	215.2	59.5	23.5	178.8	3.0	18
1.875	0.421	5.000	30.6	5.081	315.0	-1.359	313.4	78.0	24.7	259.5	1.1	13
1.890	0.413	5.097	15.1	5.110	236.5	-1.350	207.3	45.1	26.2	211.6	1.7	19
1.910	0.433	4.980	15.2	6.355	328.0	-1.574	412.6	32.0	33.1	331.6	2.6	16
1.930	0.330	5.023	30.7	5.433	612.4	-1.621	175.5	109.0	123.0	947.5	3.6	18
1.950	0.465	5.031	13.5	5.773	225.7	-0.325	43.2	36.0	11.7	89.5	4.1	16
1.970	0.430	5.018	15.1	6.050	663.9	-1.345	663.9	52.2	45.3	470.9	3.9	16
1.990	0.365	5.109	25.4	5.544	527.1	-2.319	825.9	88.5	75.4	573.5	3.3	12

Table III: Results of the fits for  $\epsilon \leq 0.6$

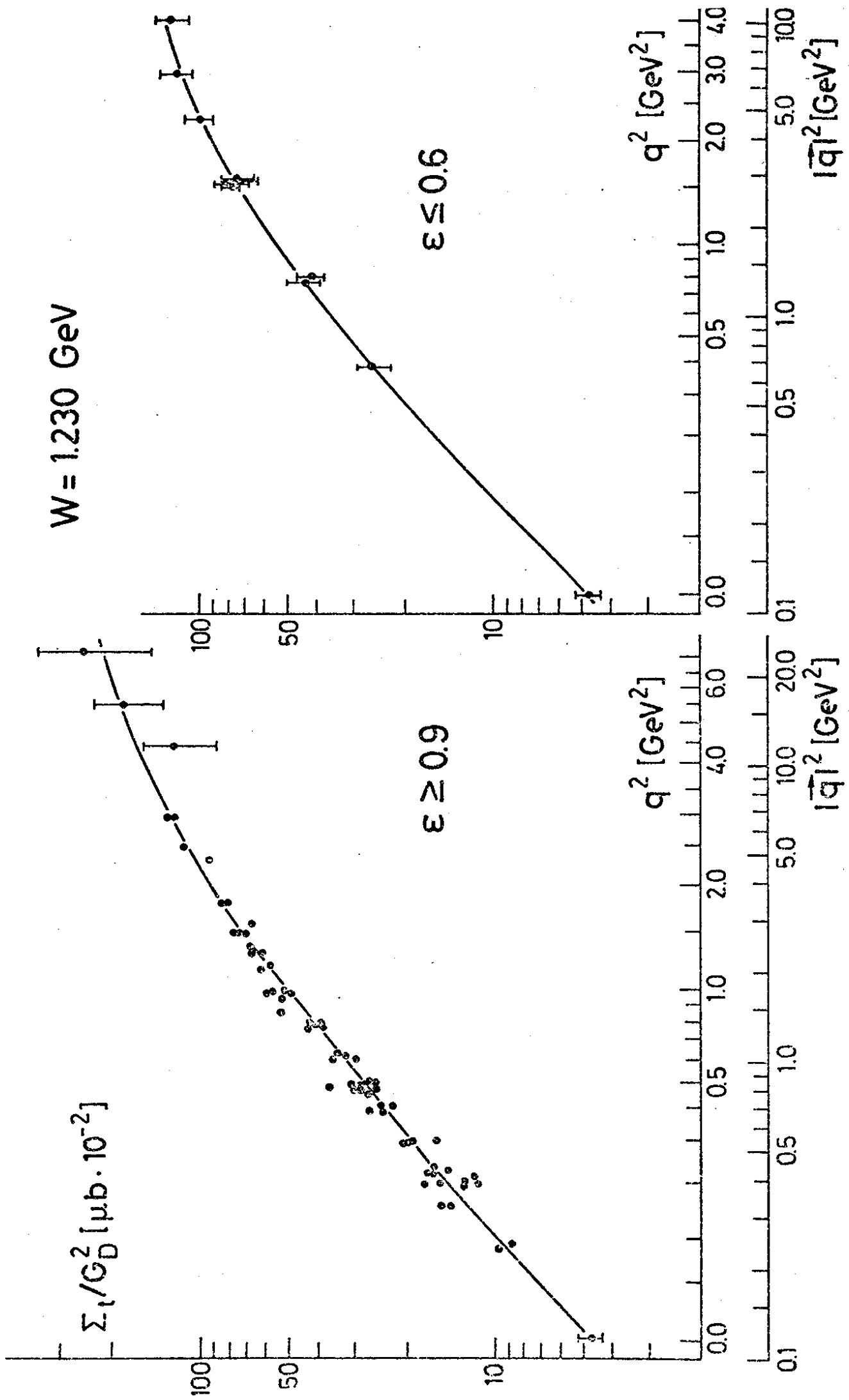


Fig. 1

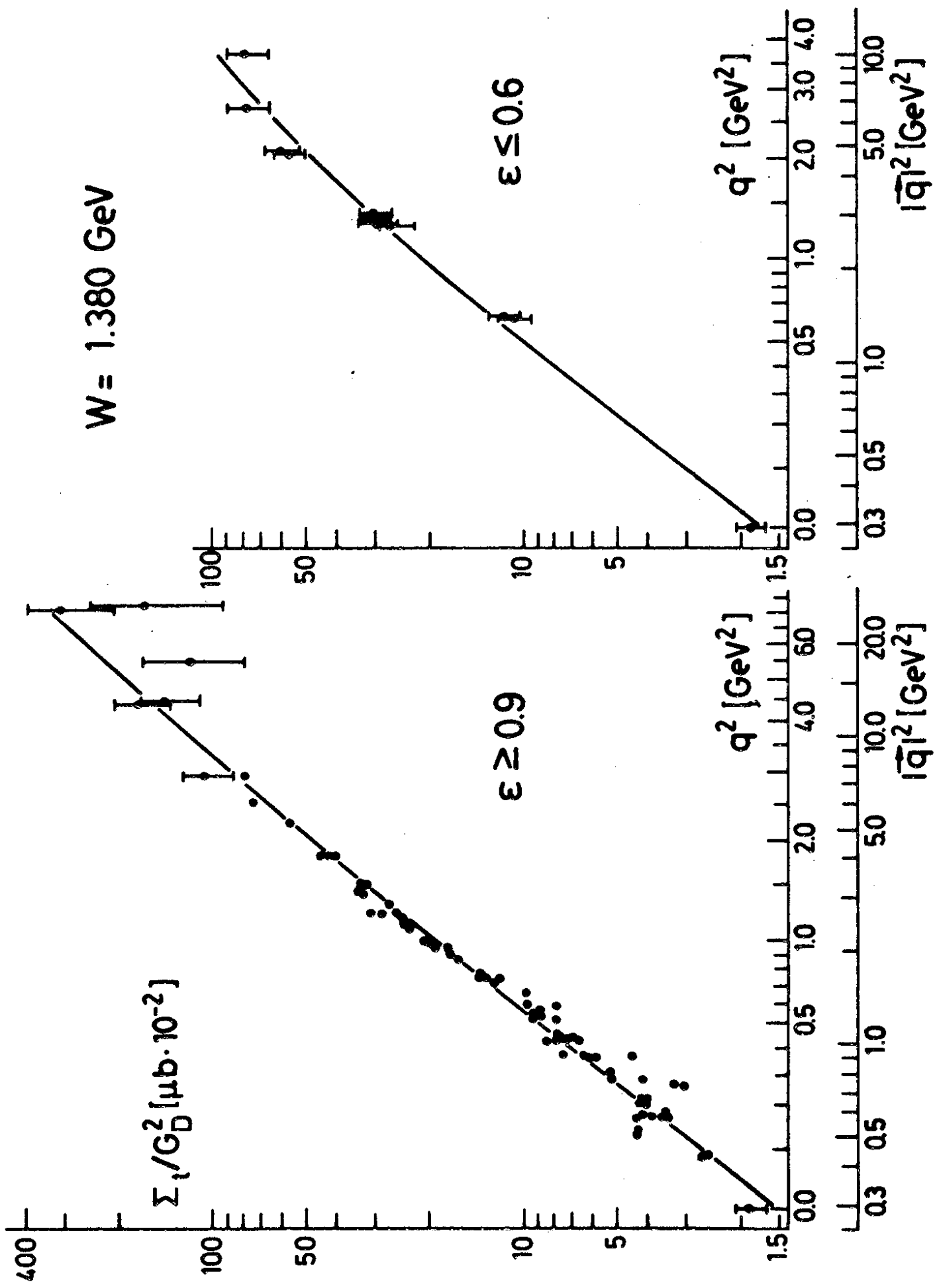


Fig. 2

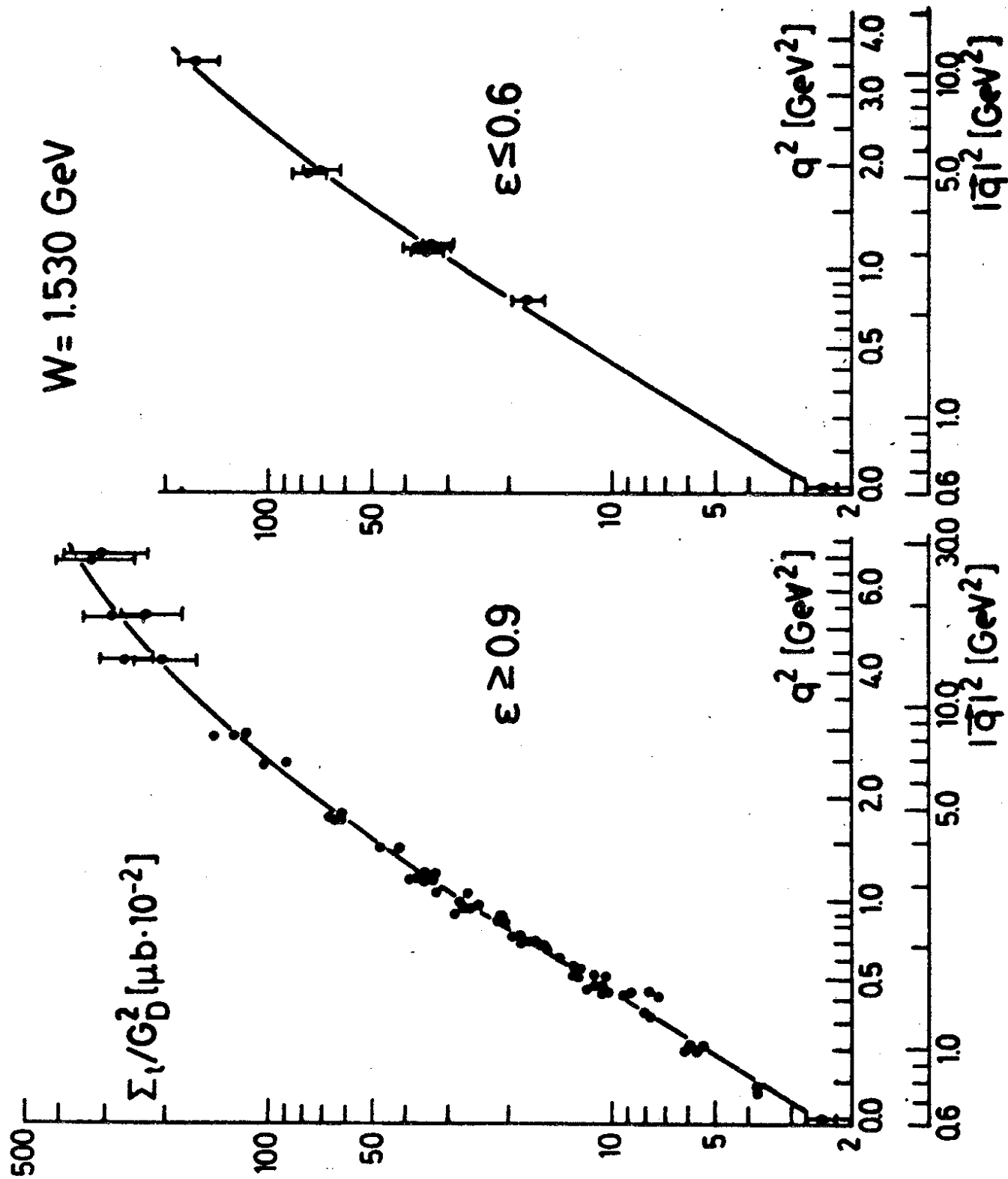


Fig.3

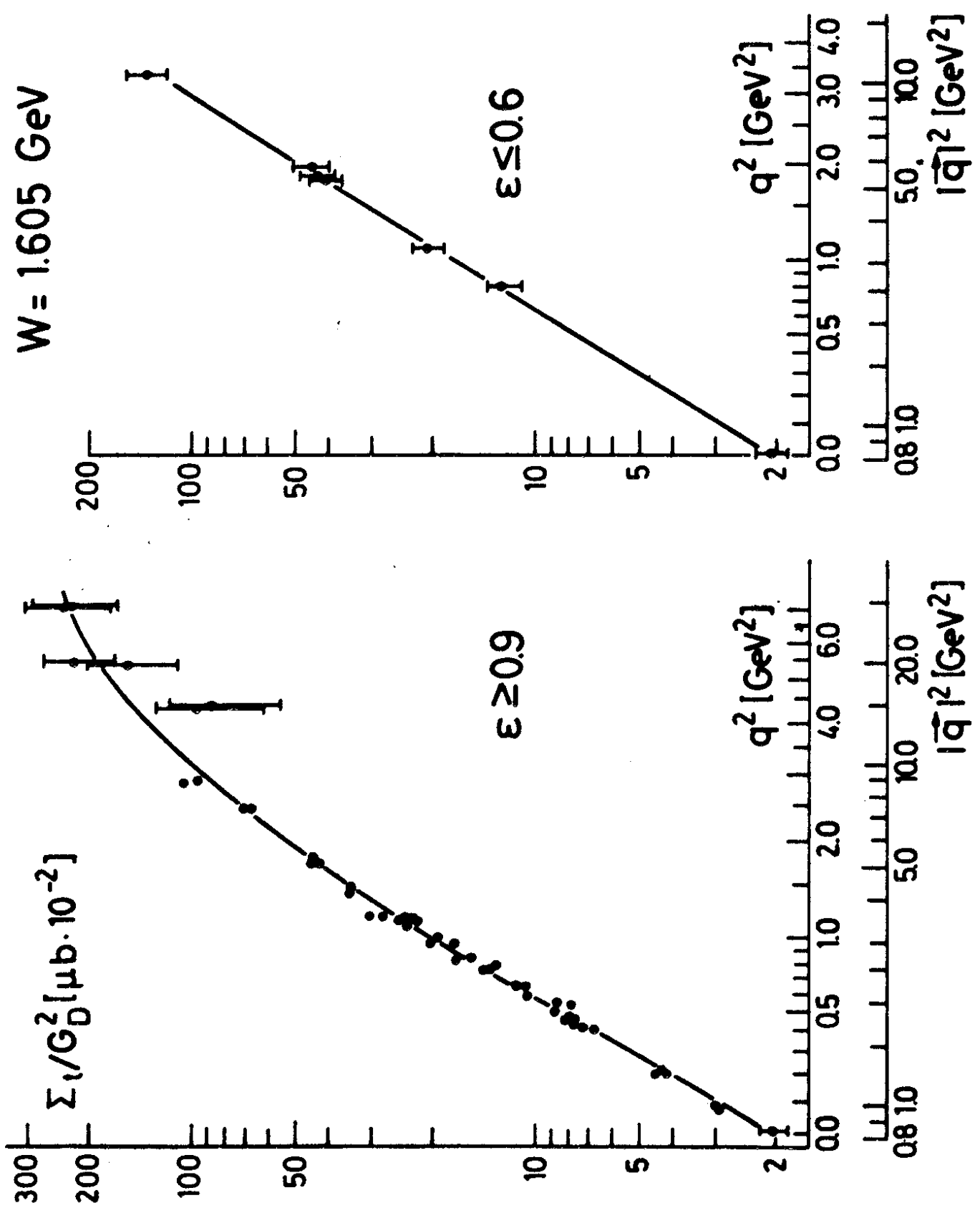


Fig. 4

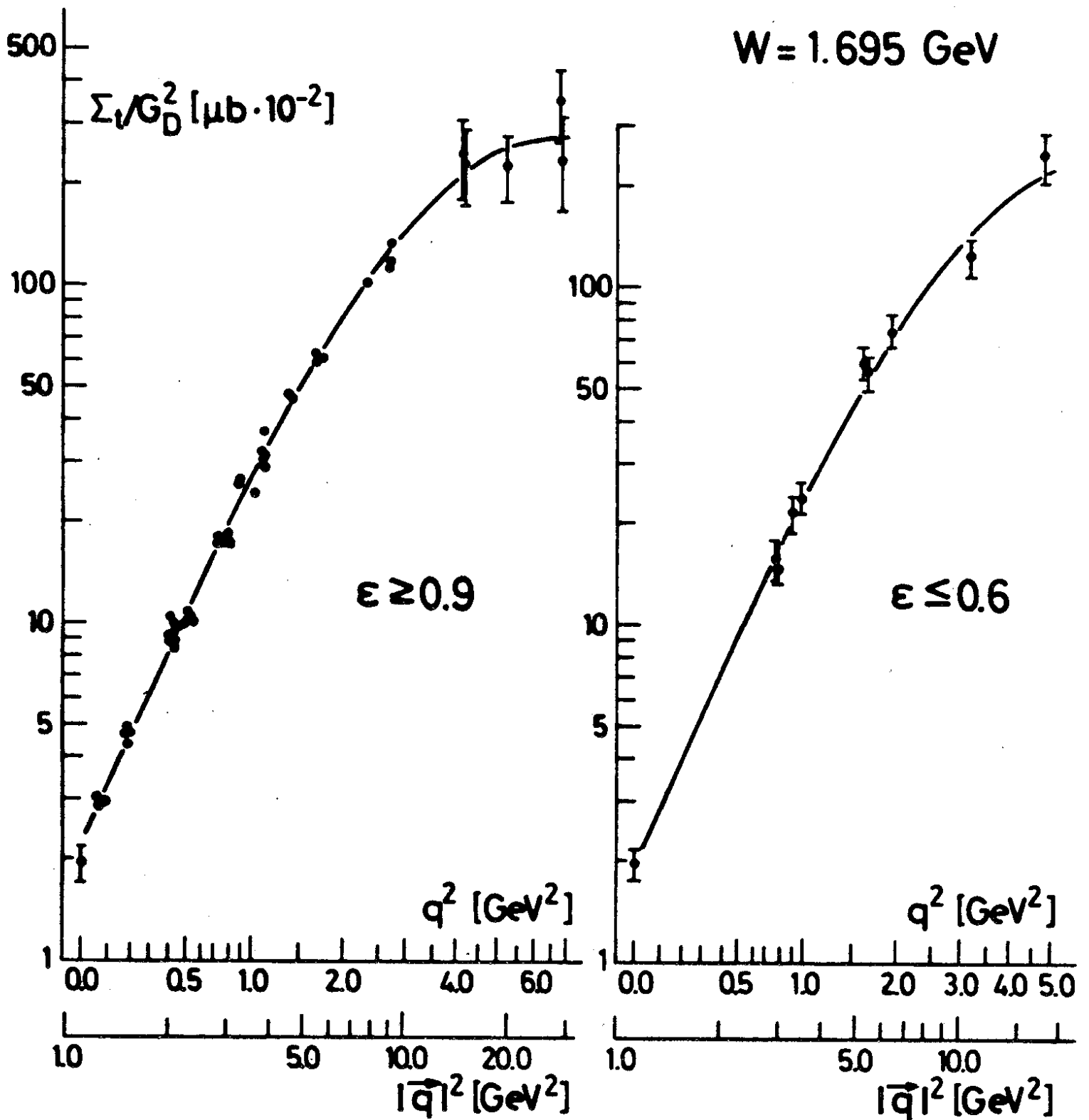


Fig. 5

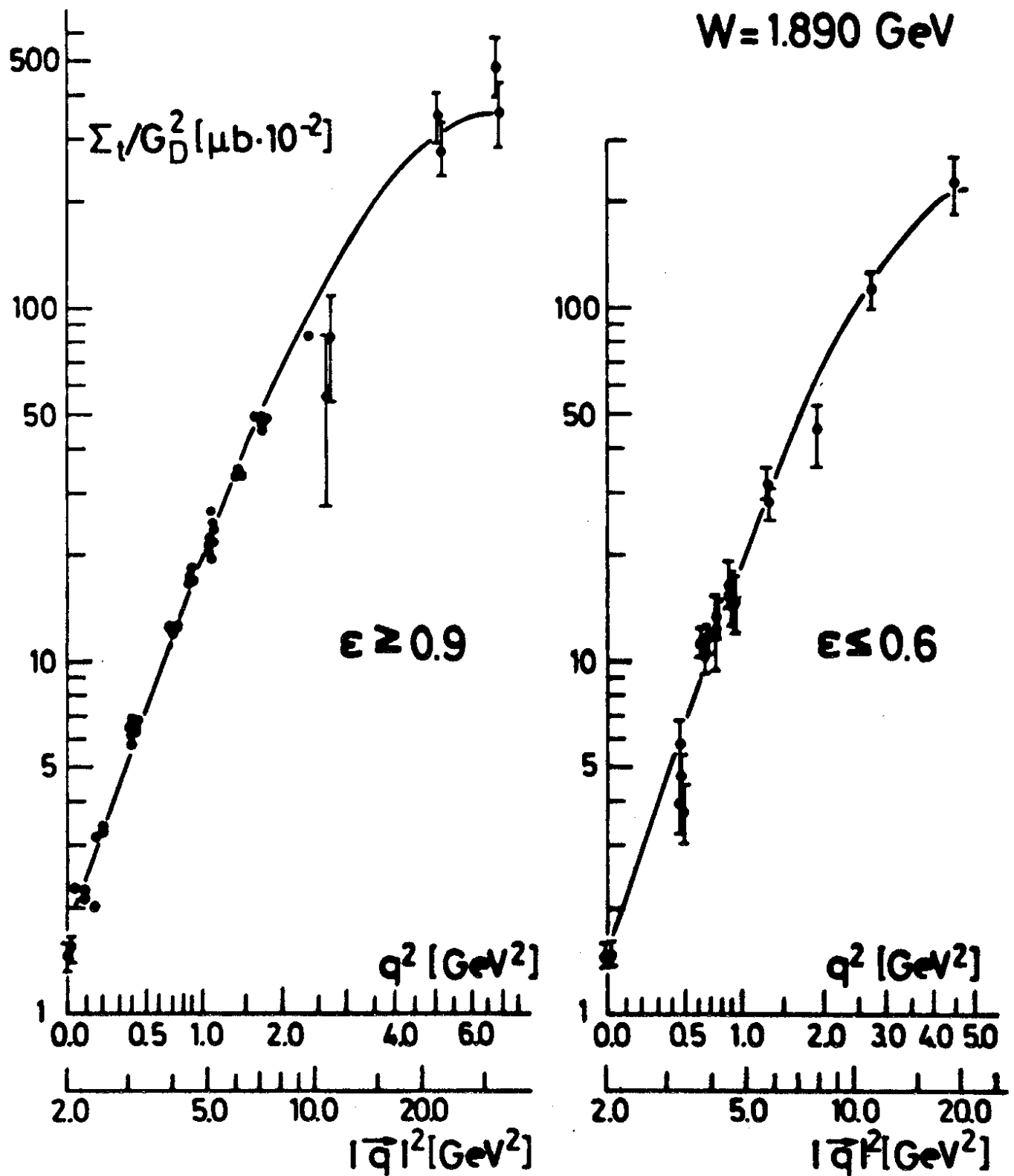


Fig. 6



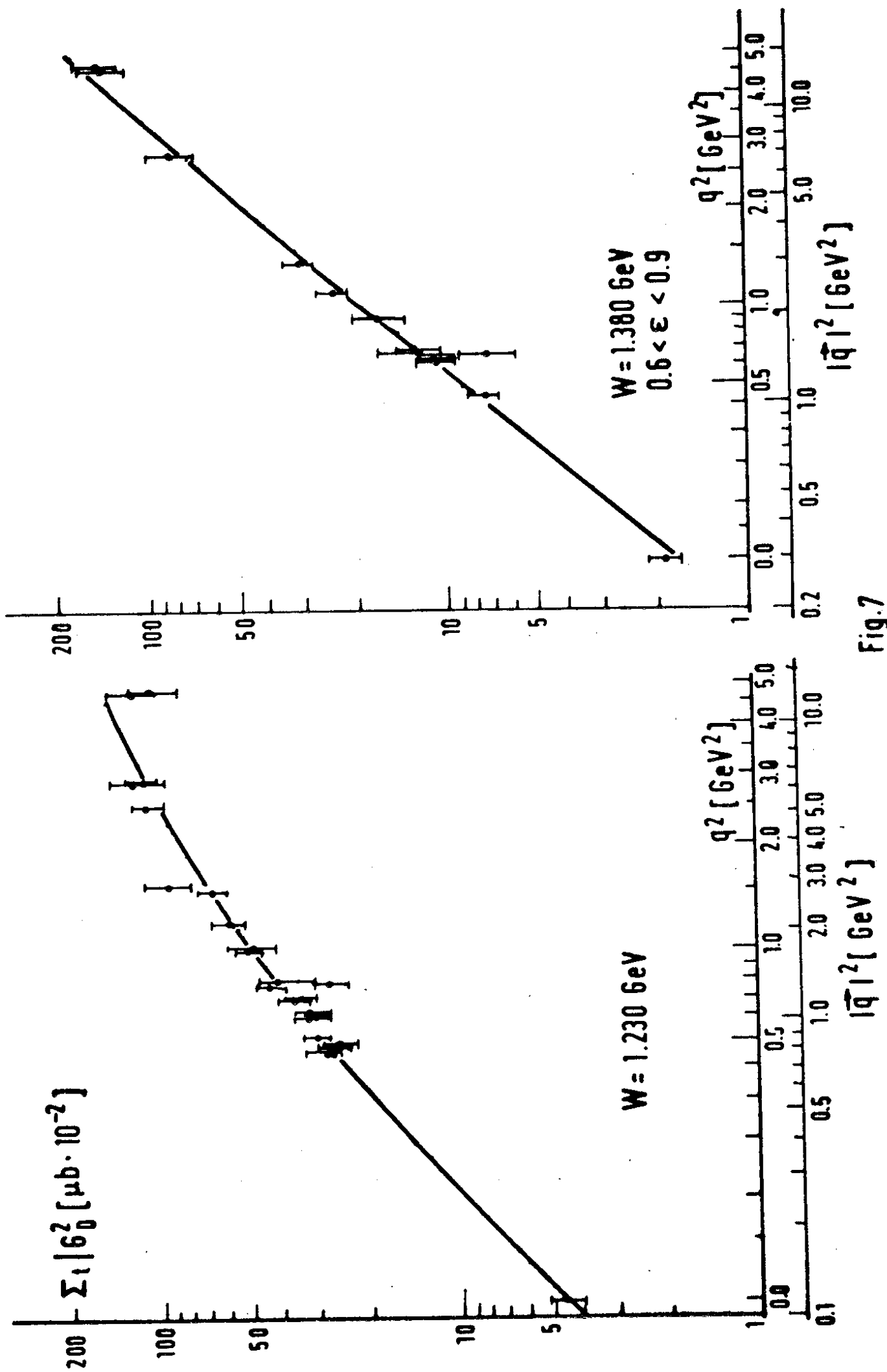


Fig.7

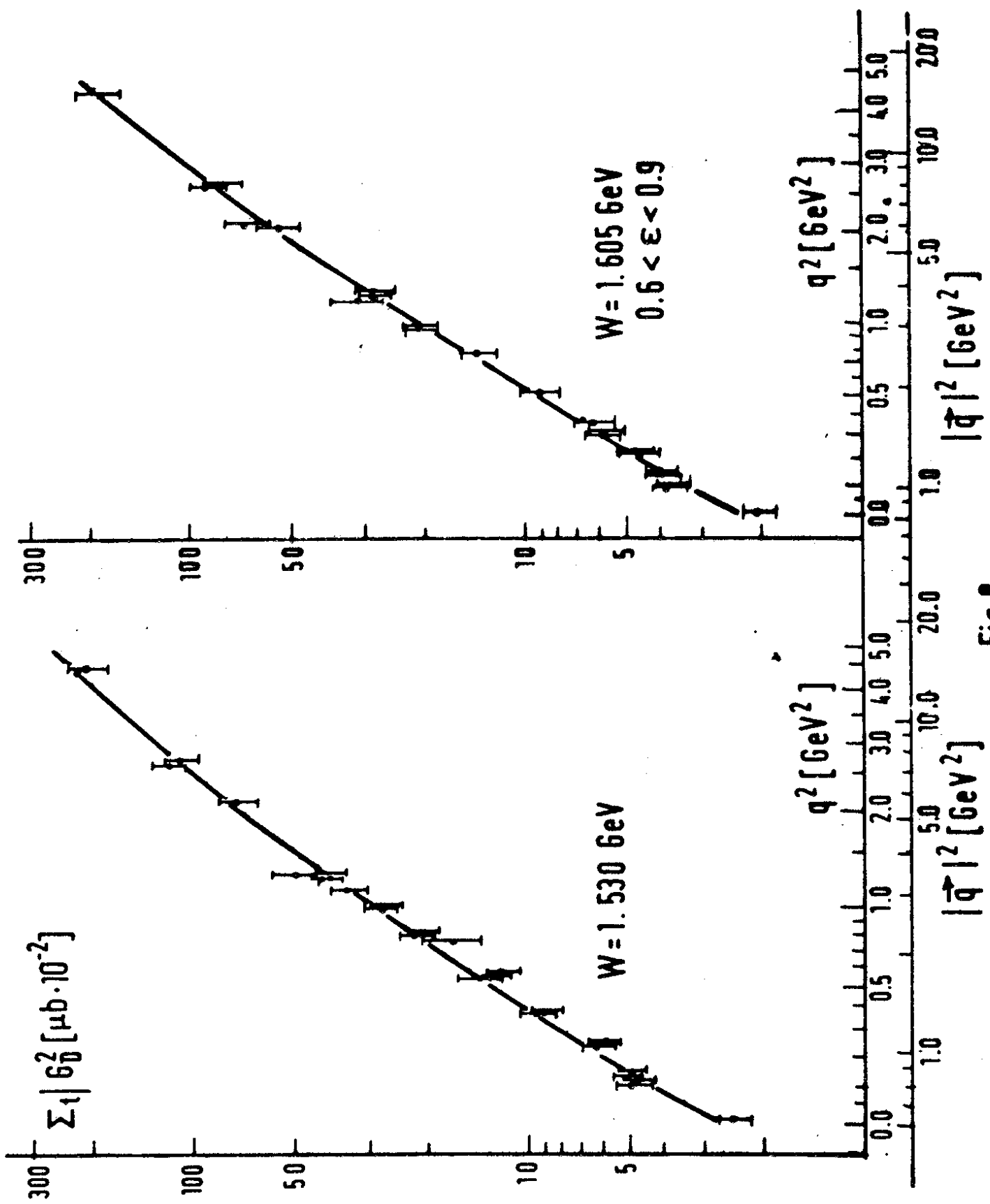


Fig. 8

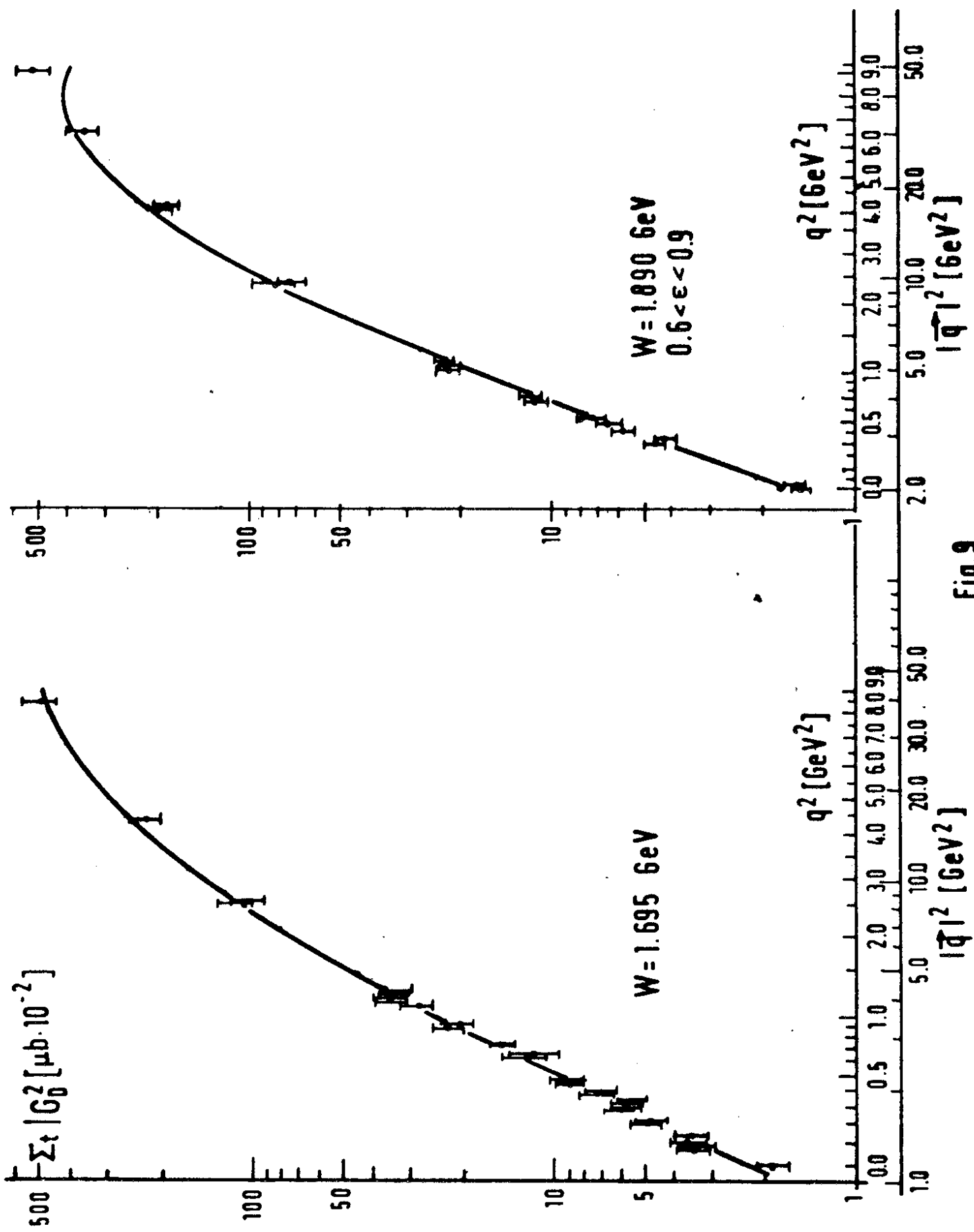


Fig. 9

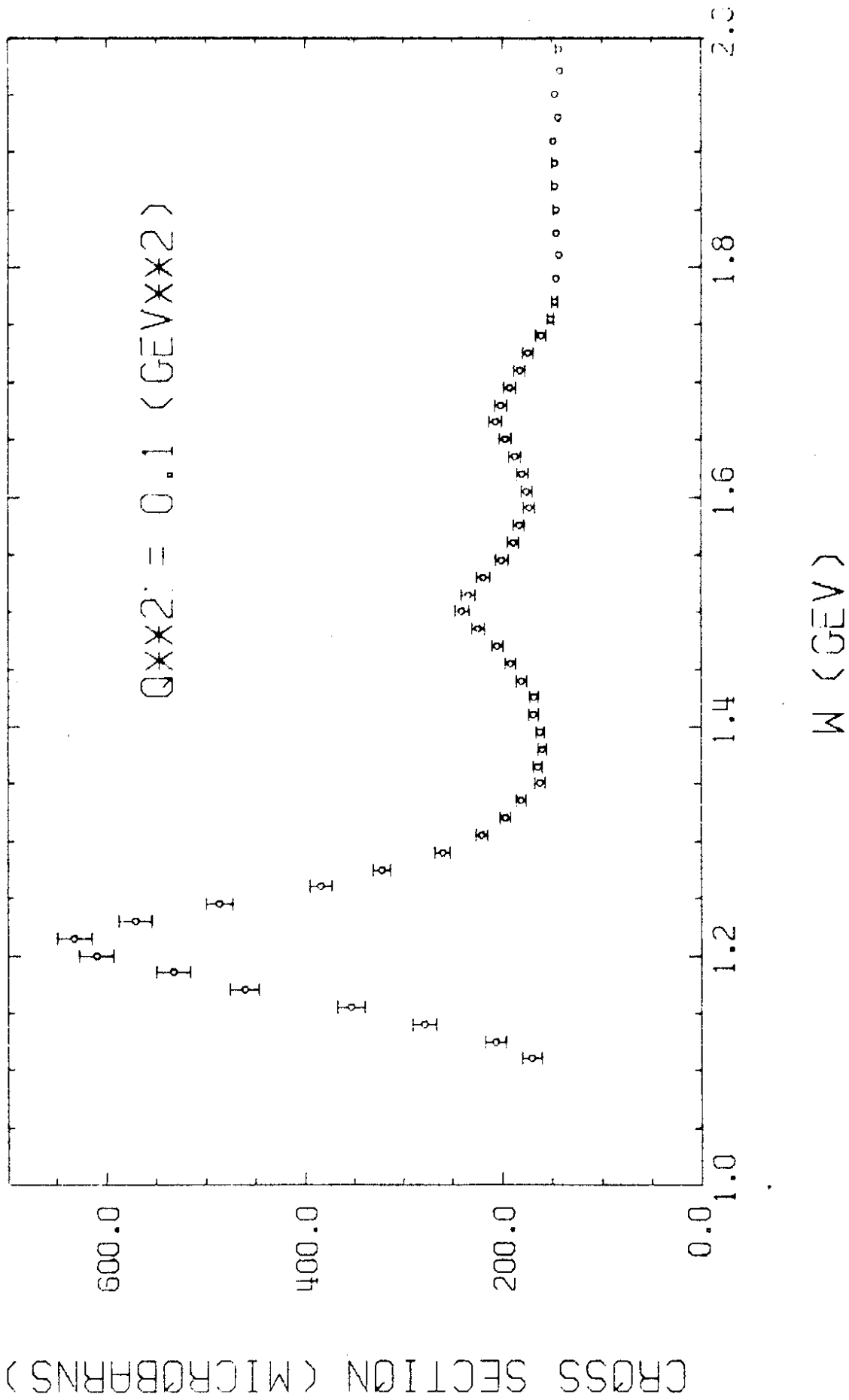


FIG. 10

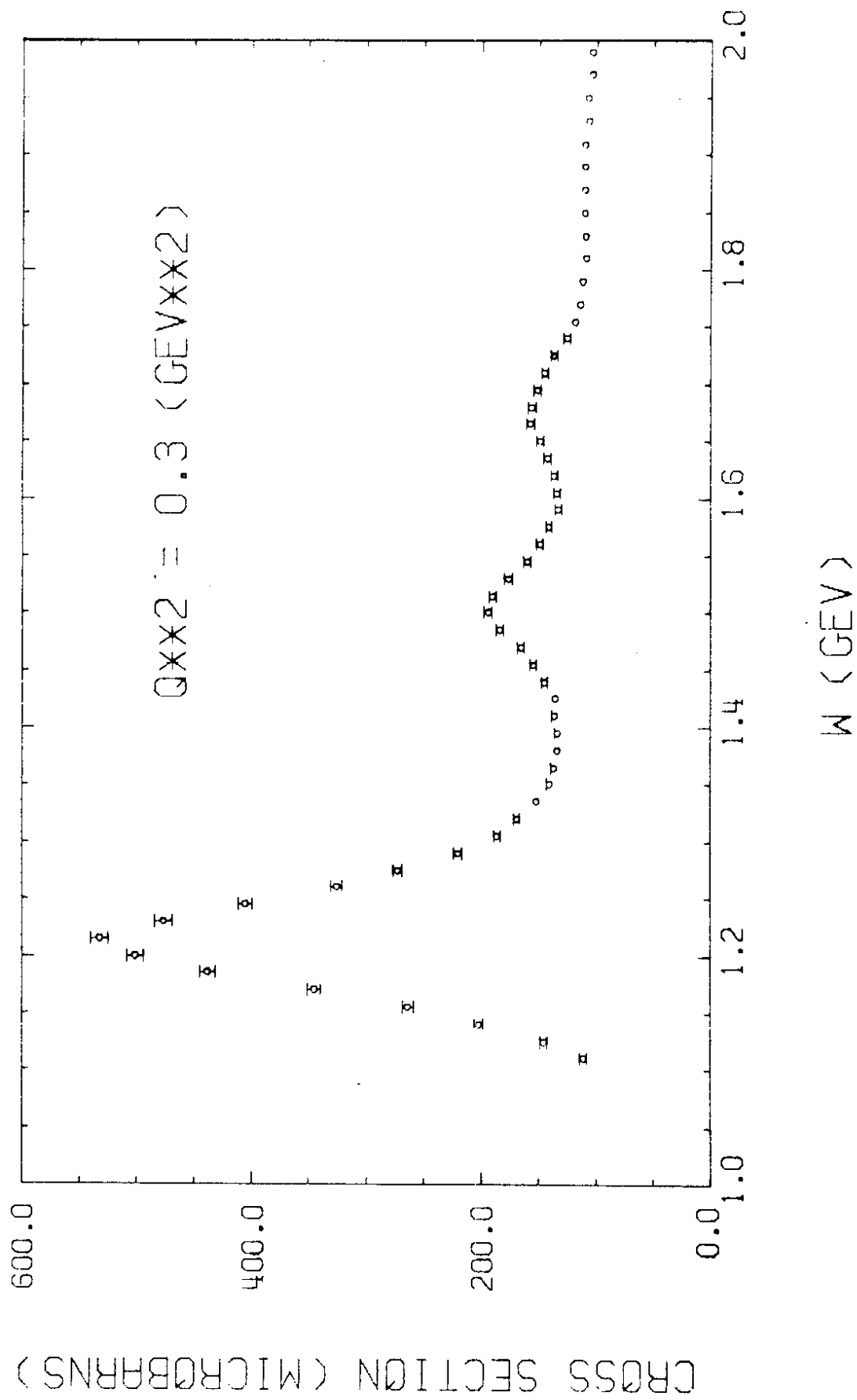
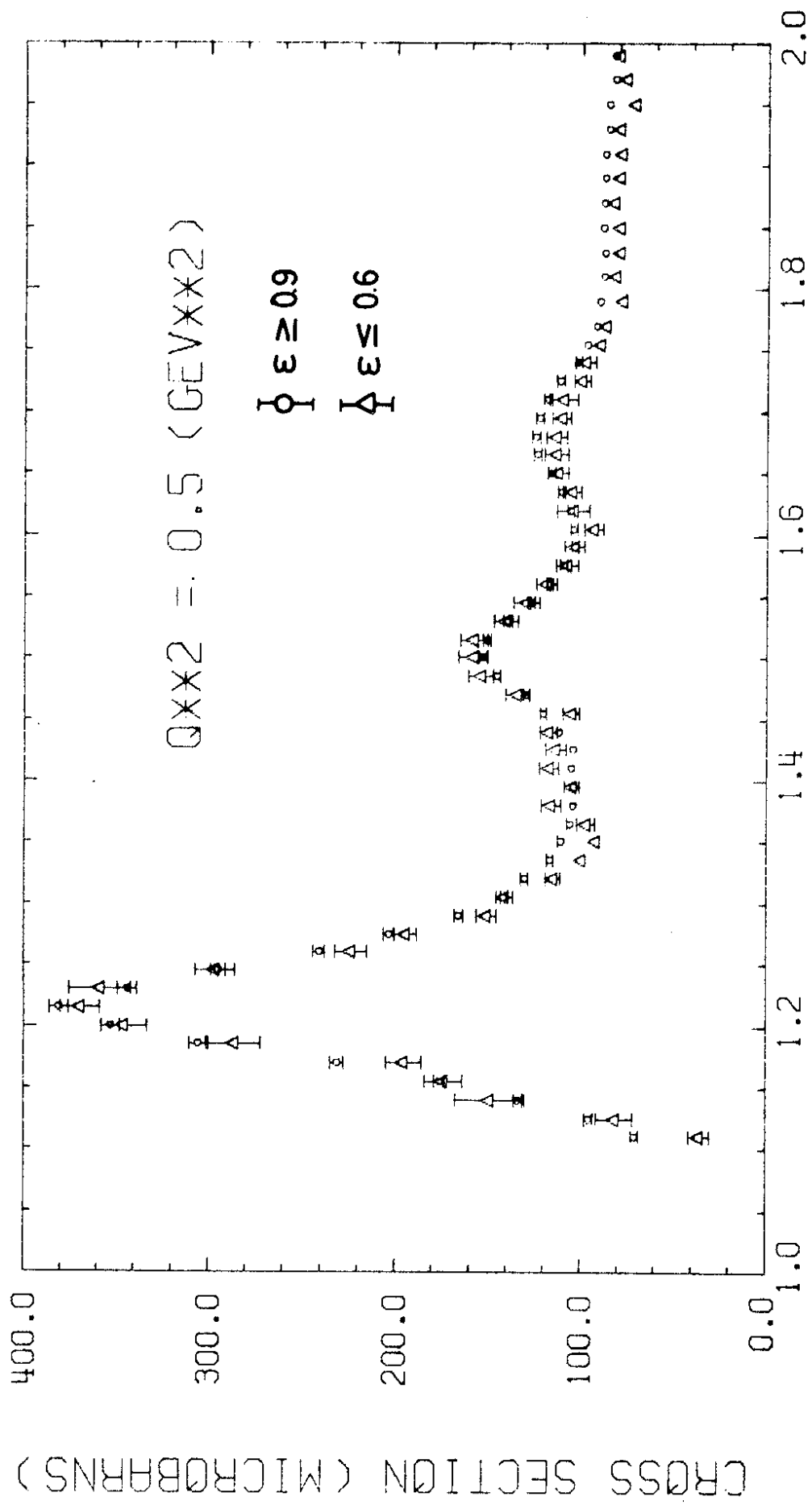
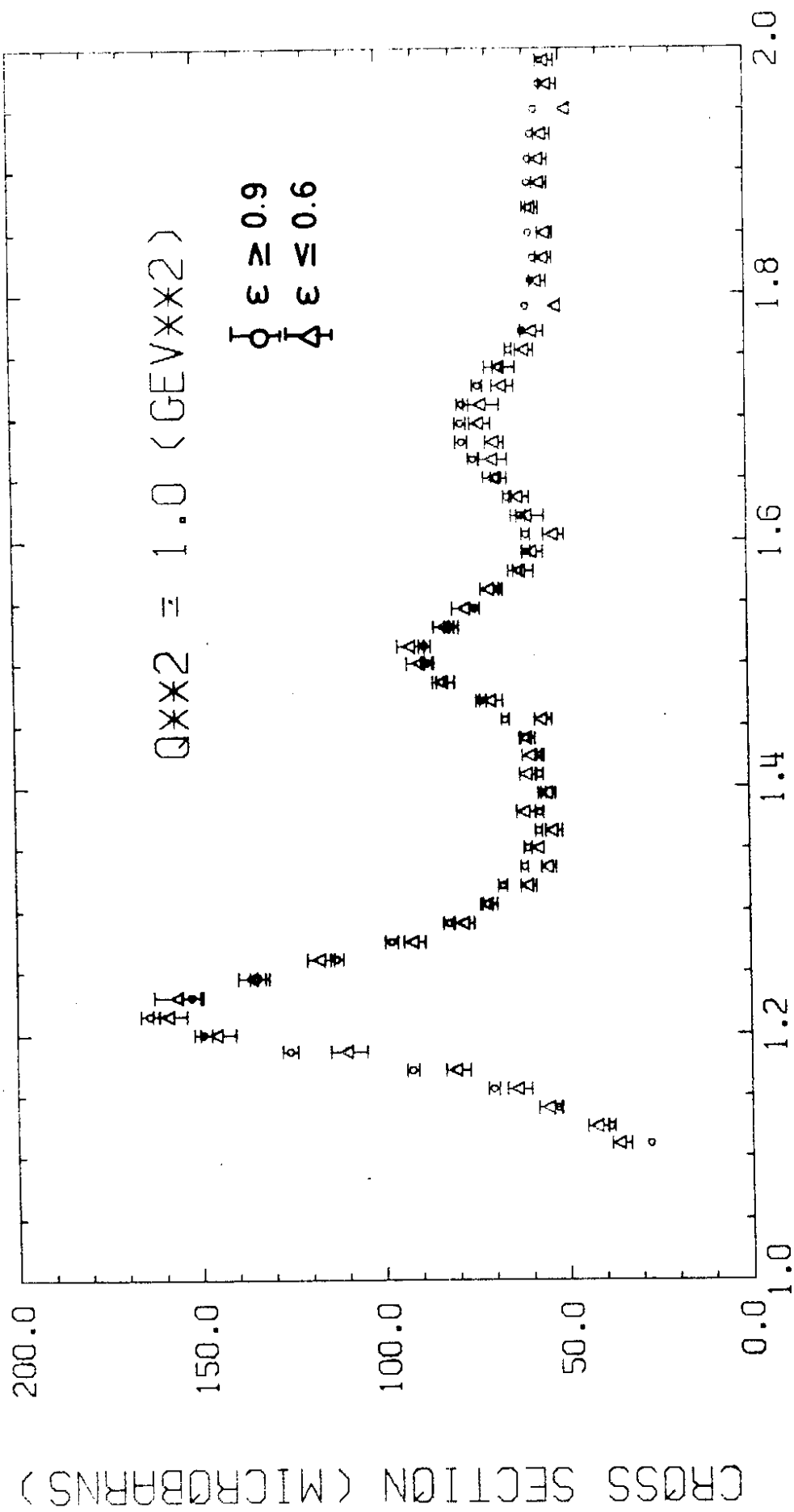


FIG. 11



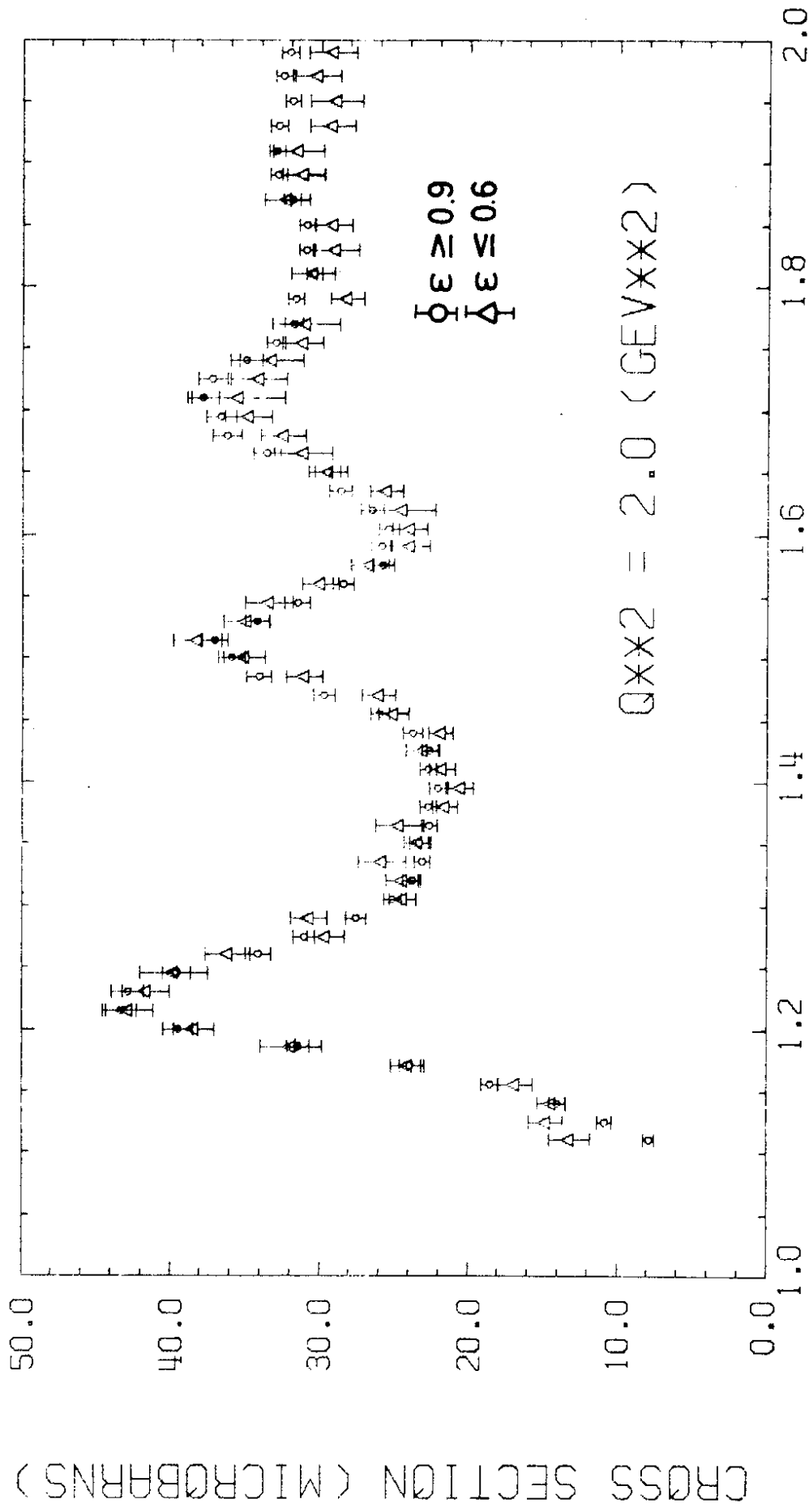
W (GEV)

FIG. 12



W (GEV)

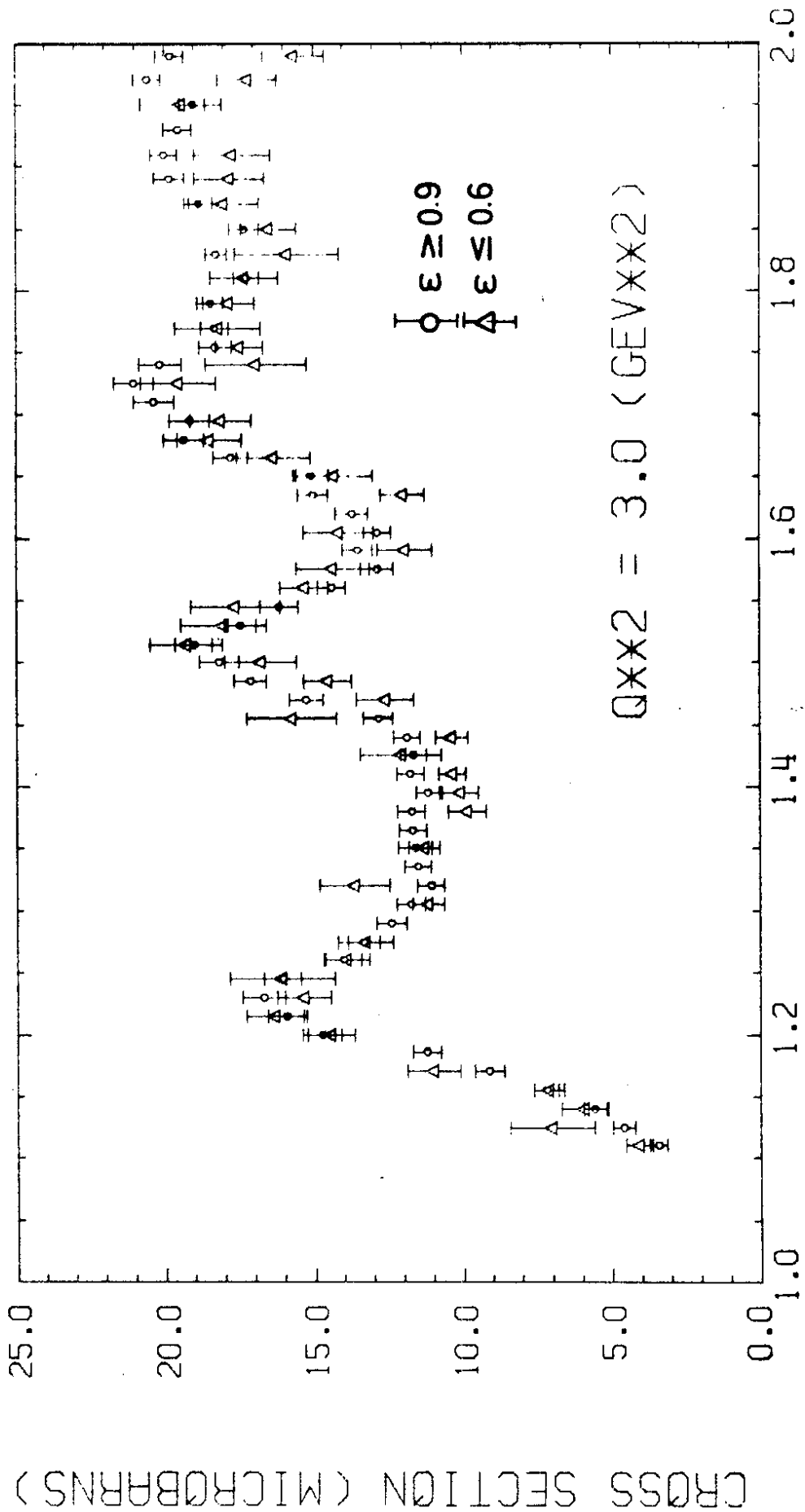
FIG 13



W (GEV)

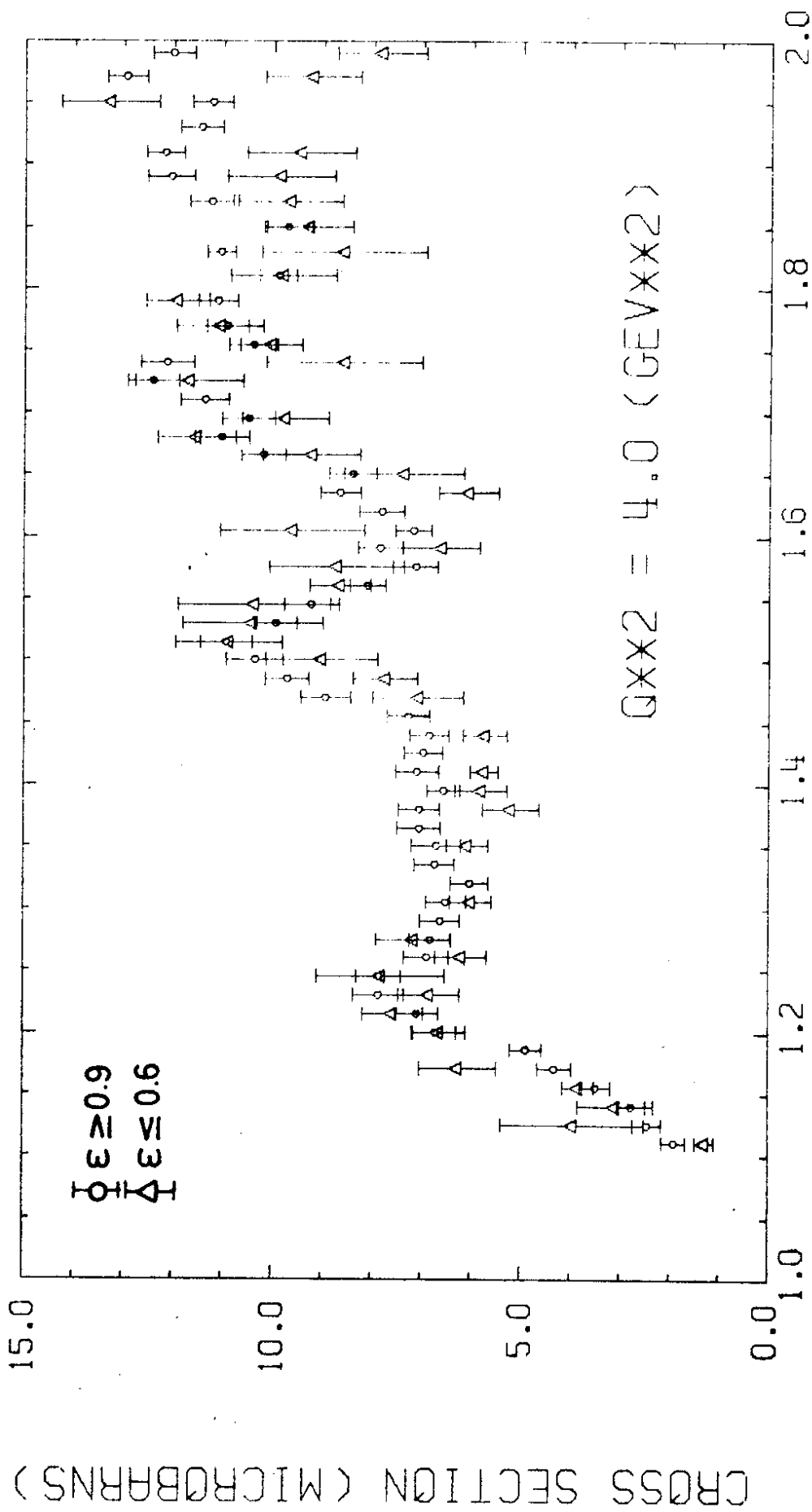
FIG 14





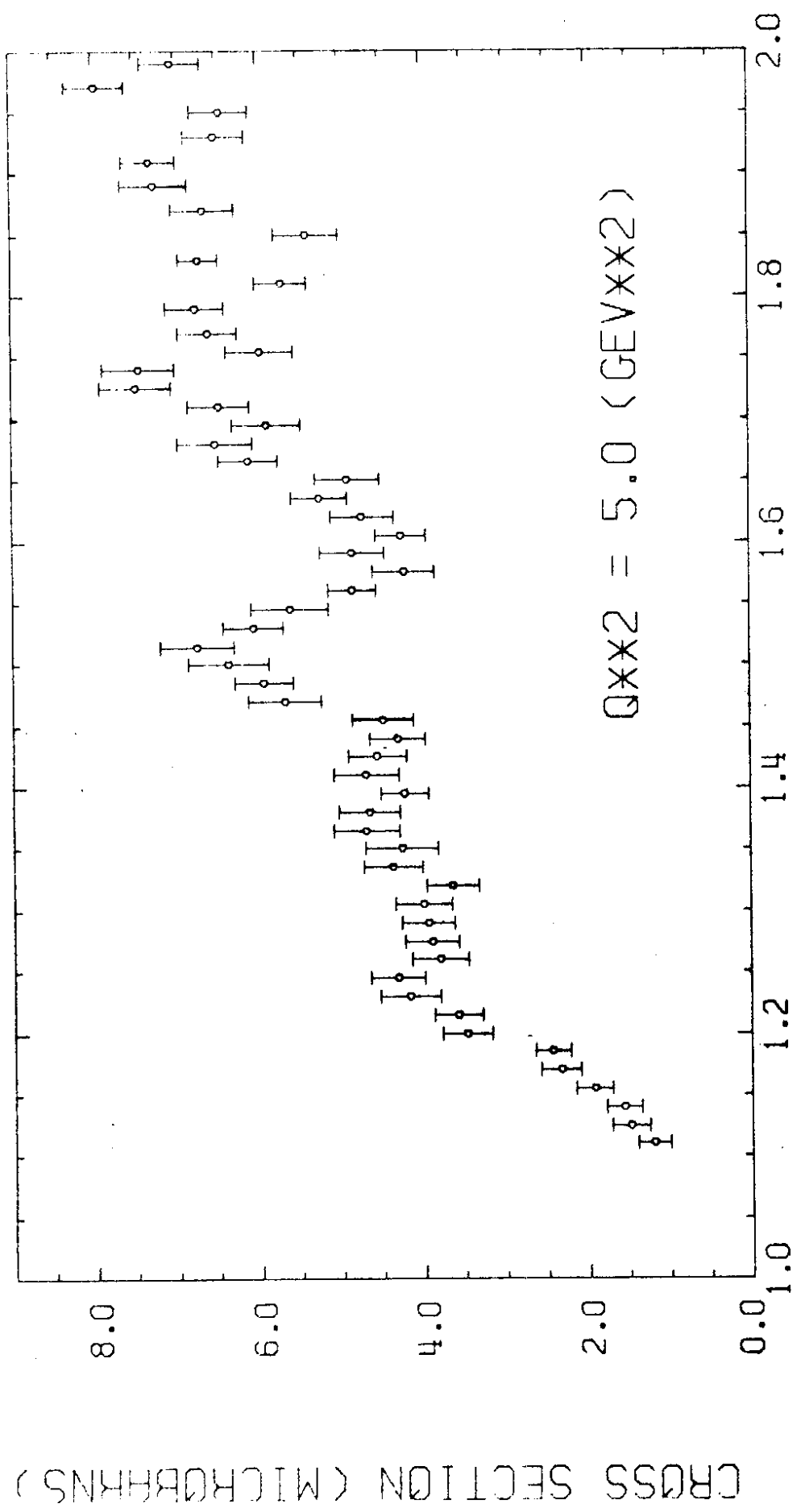
W (GEV)

FIG 15



W (GEV)

FIG 16



W (GEV)

FIG 17

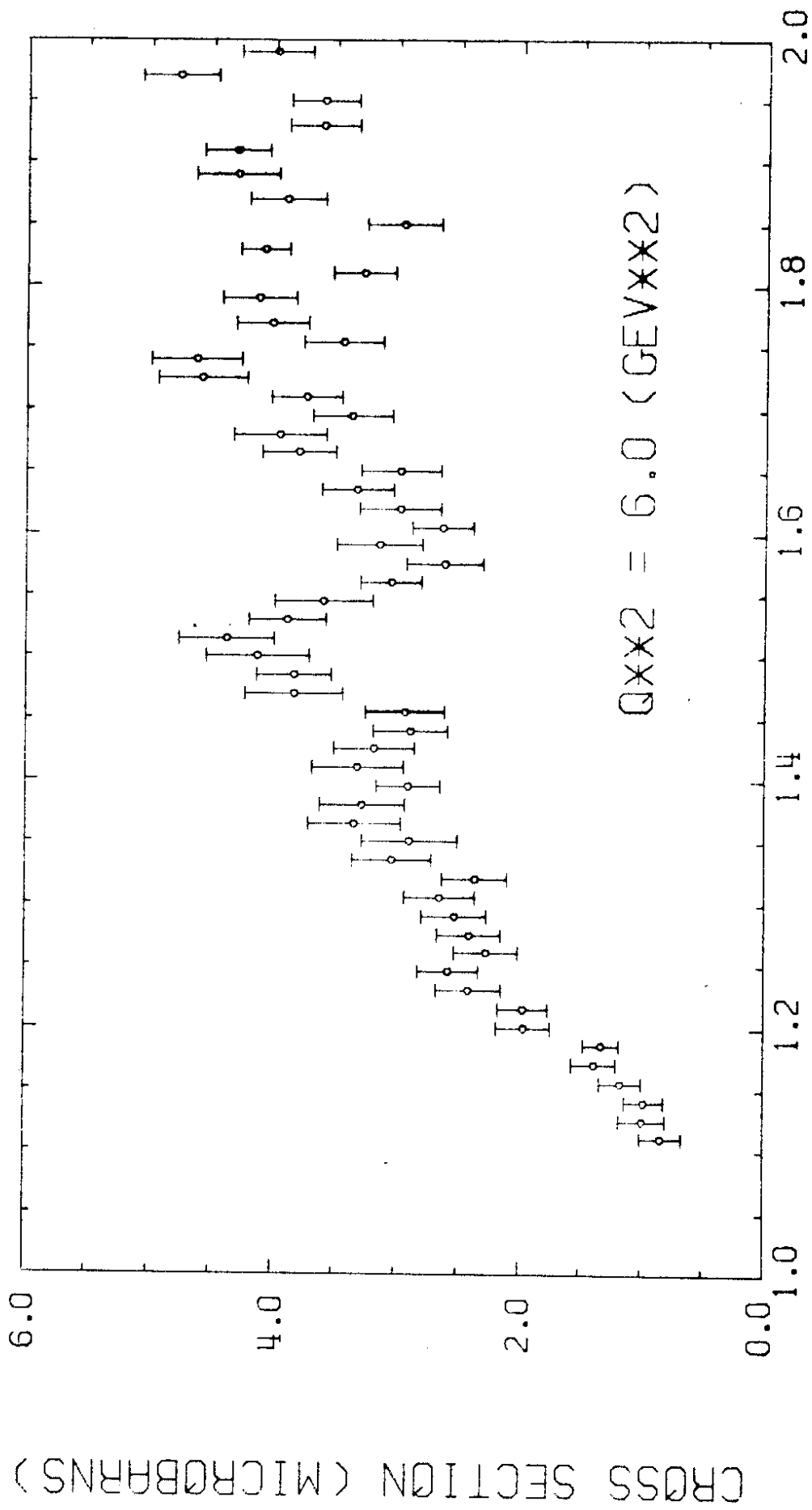


FIG 18